Adaptive Sliding Mode Control for Suspended Payload with Helicopter

Author

HASSAAN AFZAL

00000118999

Supervisor

DR. FAHAD MUMTAZ MALIK

DEPARTMENT OF ELECTRICAL ENGINEERING

COLLEGE OF ELECTRICAL & MECHANICAL ENGINEERING

NATIONAL UNIVERSITY OF SCIENCES AND TECHNOLOGY

ISLAMABAD

Adaptive Sliding Mode Control for Suspended Payload with Helicopter

Author

HASSAAN AFZAL

00000118999

A thesis submitted in partial fulfillment of the requirements for the degree of

MS Electrical Engineering

Thesis Supervisor:

DR. FAHAD MUMTAZ MALIK

Thesis Supervisor's Signature: _____

DEPARTMENT OF ELECTRICAL ENGINEERING

COLLEGE OF ELECTRICAL & MECHANICAL ENGINEERING

NATIONAL UNIVERSITY OF SCIENCES AND TECHNOLOGY, ISLAMABAD

DECLARATION

I certify that this research work titled "*Adaptive Sliding Mode Control for Suspended Payload with Helicopter"* is my own work. The work has not been presented elsewhere for assessment. The material that has been used from other sources it has been properly acknowledged / referred.

Signature of Student

HASSAAN AFZAL

118999

LANGUAGE CORRECTNESS CERTIFICATE

This thesis has been read by an English expert and is free of typing, syntax, semantic, grammatical and spelling mistakes. Thesis is also according to the format given by the university.

Signature of Student

HASSAAN AFZAL

118999

Signature of Supervisor

COPYRIGHT STATEMENT

ACKNOWLEDGEMENTS

I would like to thank my thesis supervisor, GEC committee members, my colleagues and my family who always supported and helped me whenever I need them. Especially I would acknowledge the effort of my parents who always remain a source of motivation for me. Secondly I appreciate my supervisor guidance without which I could not achieve success in completing thesis.

I dedicate this thesis to all my family members

ABSTRACT

Helicopters are utilized in transporting slung load from one place to another. They are also used in military and surveillance applications. During earthquakes and floods helicopters are used to delivering food and water supplies to remotely affected areas which are inaccessible via land maneuvering. They are also used in recuse operations. In spite of all these applications with suspended load they are more prone to vibrations because of load behavior. Load act as pendulum resulting in disturbing the control of helicopter and distracting the stability of helicopter.

This research work aims to stabilize unmanned helicopter and slung load during hovering in the presence of external disturbances and rotor downwash. Sliding mode control is applied to the helicopter to attain desired response. Linear matrix inequality based SMC is used to stabilized payload because of relatively effective problem solving ability and robustness.

Keywords: Miniature unmanned helicopter, Sliding Mode Control (SMC), Payload stabilization, Rotor downwash, Hovering, Wind gusts, Linear Matrix Inequality (LMI).

TABLE OF CONTENTS

LIST OF FIGURES

LIST OF TABLES

ACRONYMS LIST

VTOL	Vertical Take Off & Landing
SMC	Sliding Mode Control
LMI	Linear Matrix Inequality
UAV	Unmanned Aerial Vehicle
DoF	Degree of Freedom
AoA	Angle of Attack
RPM	Revolutions per Minute
LQR	Linear Quadratic Regulator
PID	Proportional Integral Derivative
RC	Remote Control
TPP	Tip Path Plane

LIST OF SYMBOLS

u_{col}	Collective control input
u_{cyc}/u_{ped}	Cyclic control input
u_{long}	Longitudinal control input
u_{lat}	Lateral control input
M	Mass of helicopter
m	Mass of attached payload
v_i	Induce velocity
T	Thrust of main rotor
L	Lift of rotor
u	Longitudinal linear velocity
v	Lateral linear velocity
w	Vertical linear velocity
p	Roll angular velocity
q	Pitch angular velocity
r	Yaw angular velocity
ϕ	Roll angle
Θ	Pitch angle
Ψ	Yaw angle
a	Longitudinal flapping angle
b	Lateral flapping angle
S	Surface area of volume surrounding rotor and wake
dS	Normal unit area vector to volume surrounding rotor and wake
A	Area of rotor disk
s	Sliding surface
V	Lyapunov function

CHAPTER 1: INTRODUCTION

1.1 Background and Motivation

Unmanned vehicles have gained focus of research in the recent few years since they can be controlled from far off place via Remote Control (RC), minimizing human pilot life loss. Even these vehicles are capable of performing autonomous maneuvers. With the advancement in technology especially in case of artificial intelligence, vehicles become more independent resulting in reducing dependency over human control. In spite of their valuable uses and prime importance, control development for these vehicles has become enormous challenge due to uncertainties and external disturbances. In case of unmanned aerial vehicles control development become even more difficult due to complex mathematical model. Even aerial vehicles require stabilizing themselves at particular height before performing any maneuver. These all factors make unmanned aerial vehicles prime research interest for engineers.

Helicopters utilization scope comprises of reconnaissance as well as rescue applications. Unlike fixed wings aircrafts they are capable of hovering and vertical takeoff & landing. Due to vast range uses and multitasking capabilities world has shifted focus of research towards helicopters. However external disturbances are the major threat to helicopter stability. These disturbances not only effect helicopter but induces pendulum like swing in attached load which creates an additional destabilizing source for the system. Under these circumstances if vibrations are not neutralized fatal accidents can occur.

In addition to time varying air disturbances another form of disturbance is induced in helicopters called rotor downwash. During rotation, helicopter rotor interact with air around blades and induces a velocity called induce velocity. This velocity trails down slowly causing variable air loads on blades which decreases efficiency of blades by inducing vibrations in systems. If rotor downwash effects are not minimized they may result in fatal accidents. Hence suppressing effects of rotor downwash is necessary for attaining smooth and effective performance of helicopter.

On the basis of structure and functioning helicopters are divided into following categories. All these type of helicopters have their own capabilities, uses as well as draw backs. Figure 1.1 shows few types of helicopters.

1. Tandem-rotor helicopter

   These helicopters have two sets of rotor blades. Both of these rotors play their role controlling thrust and direction of helicopter. Both rotors are controlled by different control input. They use less power during hovering. They can handle weight of helicopter with blades of short length however aerodynamics of front rotor significantly affect the back rotor performance.

2. Coaxial helicopter

   These helicopters also have two sets of rotating blades but both rotors are controlled by single input. They can handle heavy payloads with same power as compared to single rotor helicopters but they are more prone to mechanical wear.

3. Notar helicopter

   Nortar helicopters are similar to single rotor helicopter but they lack tail rotor unlike to single rotor helicopters. Such vehicles comprise of fixed wing at their as a replacement of tail rotor. They are less affected by mechanical wear due to absence of tail rotor and gearing between two rotors. They create less noise but these vehicles are not fuel efficient.

4. Tilt rotor helicopter

   These aerial vehicles have capabilities of both helicopters and aero-planes. They can takeoff from ground like helicopter and can fly like an aero-plane. In this way landing and takeoff time can be reduced. They are capable of attaining high speeds but at cost of reducing payload attached with it

5. Single rotor helicopter

   Single rotor helicopters are most common type of helicopters. Usually helicopters comprise of two rotors. Tail rotor thrust is used to control the direction of flight in terms of controlling yaw moment. It is also responsible to nullify the effect of main rotor torque. Main rotor is responsible generating thrust which controls the vertical distance (height) of aerial vehicle from reference point. Thrust is controlled in following ways

a) By changing revolutions per minute.
b) By changing angle of attack of main rotor.

Usually first method is not preferred since changing RPM require more time in achieving thrust due to large inertia of blades. For increasing or decreasing thrust of helicopter pitch angle of rotor blades are changed simultaneously and input responsible for such motion is

called **collective control input ($\mathbf{u_{col}}$)**. In order to move helicopter forward or side-ways pitch angle of helicopter main rotor is changed in required direction. Such control input is called **cyclic control input ($\mathbf{u_{cyc}}$)** which represents changing pitch angle of blades non-simultaneously. Usually pitch angle is changed one time per revolution. Lateral motion is controlled by cosine while longitudinal motion is controlled by sine part of input. To avoid phase lag control input is applied little before helicopter blades achieve require direction. Such lag time is measured in terms of angle; normally phase angle of 90 degrees is considered. In forward flight main rotor is little bit tilted sideways to reject the drag force component which trends to move helicopter side-ways.

In case of tail rotor its collective control input (u_{col}) is responsible for regulating thrust of rotor. This rotor is directly connected to main rotor so its RPM cannot be changed separately. Moreover cyclic or directional control of tail rotor is also not possible. During forward flight tail rotor thrust force counters the main rotor. For turning sideways thrust force is increased or decreased depending upon the direction of main rotor torque. Normally such force acts in opposite direction to main rotor torque direction.

Other two inputs comprise of **longitudinal control input ($\mathbf{u_{long}}$)** for controlling forward motion by introducing forward pitching in the system while **lateral control input ($\mathbf{u_{lat}}$)** is used for sideways direction control by introducing roll in the system. Usually helicopter model can be divided into two subsystems due to negligible coupling between two subsystems

a) Longitudinal-lateral subsystem

   This subsystem control forward and sideways direction. It is controlled by longitudinal (u_{long}) and lateral control (u_{lat}) inputs respectively. Blade flapping motion is also controlled by these control inputs.

b) Heading and Heave subsystem

   This subsystem controls thrust generation (height from surface of earth) and yaw angle of helicopter (direction of flight). Collective control input (u_{col}) controls thrust generation of the main rotor while yaw angle is actuated by cyclic control input (u_{cyc}).

Both of these subsystems can be controlled separately and independently creating ease in control development for helicopters. In this thesis both subsystems are controlled separately by developing separate controls for each system. Control scheme for whole system is described in Chapter 3.

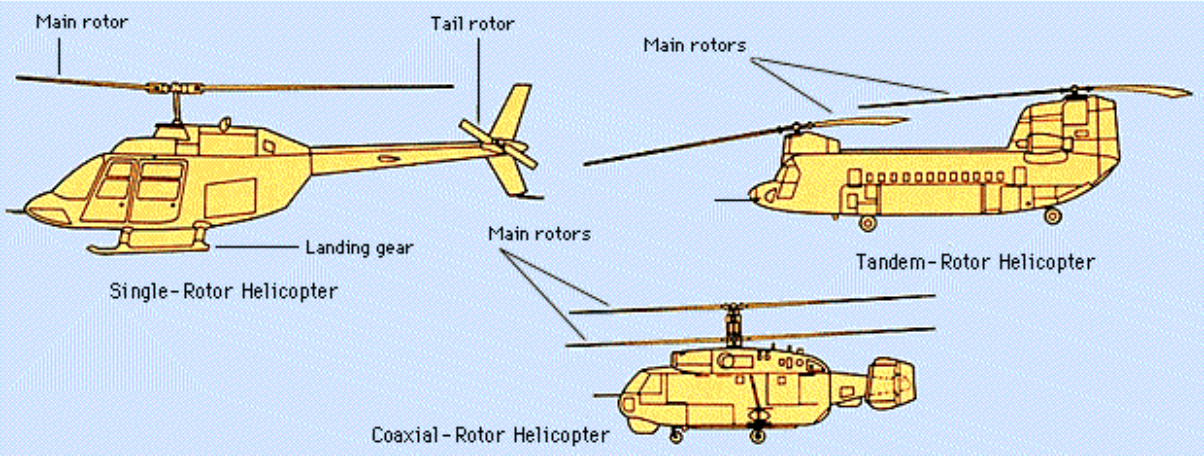

Figure 1.1: Various types of helicopters
Source: Helicopter Aerodynamics by L. Sankar

1.2 Helicopter Flight Modes

Helicopters flight modes can be divided into following types

1. **Hovering**

   In this mode helicopter maintains constant height above ground over some specific point without moving in any direction. During this operation heading also remains constant.

2. **Vertical takeoff to hover**

   It involves motion of helicopter in vertically upward direction with constant heading till point of hovering.

3. **Hovering turn**

   In this mode nose of helicopter is rotated in sideways direction while maintaining constant position and height over hovering point.

4. **Hovering leading to forward flight**

   Moving forward while maintaining constant height and heading is included in this mode. Usually this operation involves pitching helicopter main rotor in forward direction.

5. **Hovering leading to side flight**

   Moving sideways while maintaining constant height and heading is included in this mode. Usually this operation involves rolling helicopter main rotor in desired sideway direction.

6. **Hovering leading to rearward flight**

   In this mode hovering height and heading is maintained. It is similar to motion in hovering leading to forward flight but cyclic pitch is applied in backward direction.

7. **Taxiing**

   This operation involves keeping helicopter on specified taxi path. It is further divided into following three types

   a. Hover taxi is hovering forward, sideways of rearward operation which occurs above ground level and below 25 feet.
   b. Air taxi occurs between ground level and below 100 feet above ground but at greater speed than hover taxi.
   c. Surface taxi is applicable to wheeled helicopters to minimized rotor downwash effects. Collective pitch is turned to zero initially while forward cyclic pitch is applied.

8. **Takeoff from hovering**

   It is transition to forward flight by increasing altitude.

9. **Takeoff from surface**

   This mode involves moving helicopter from surface into phase of transitional lift and climb with minimum usage of power.

10. **Turning**

    This involves varying heading of helicopter.

11. **Normal climb**

    It involves increasing collective pitch.

12. **Normal descend**

    In this mode altitude of helicopter is decreased by reducing collecting pitch.

1.3 Coordinate System

Usually four types of coordinate systems are used in deriving helicopter dynamics.

1. Body frame of reference

   It has origin at center of gravity of helicopter. Positive x axis points towards longitudinal direction while positive y axis points to right lateral direction of helicopter. Positive z axis points down to center of earth.

2. Earth frame of reference

Inertial frame of reference is used while modeling by considering earth stationary and straight instead of round. Positive y axis points towards eastern side of earth while z axis points downwards. Positive x axis directs towards north.

3. Hub frame of reference

   This coordinate system exists for main as well as tail rotor. Direction of coordinate axes exist same as in body frame of reference the only difference is in location of origin which is located at hub of main rotor. In case of tail rotor similar directions are used except origin is located at tail hub.

4. Blade frame of reference

   Like previous frame of reference it also exists for tail and main rotor. Positive x axis points in back direction opposite to rotational direction of blade in blade plane. Positive y axis points in opposite direction to hub and exists along the blade while z axis exist perpendicular to blade and pointing in upward direction. Figure 1.2 shows body and earth frame of reference.

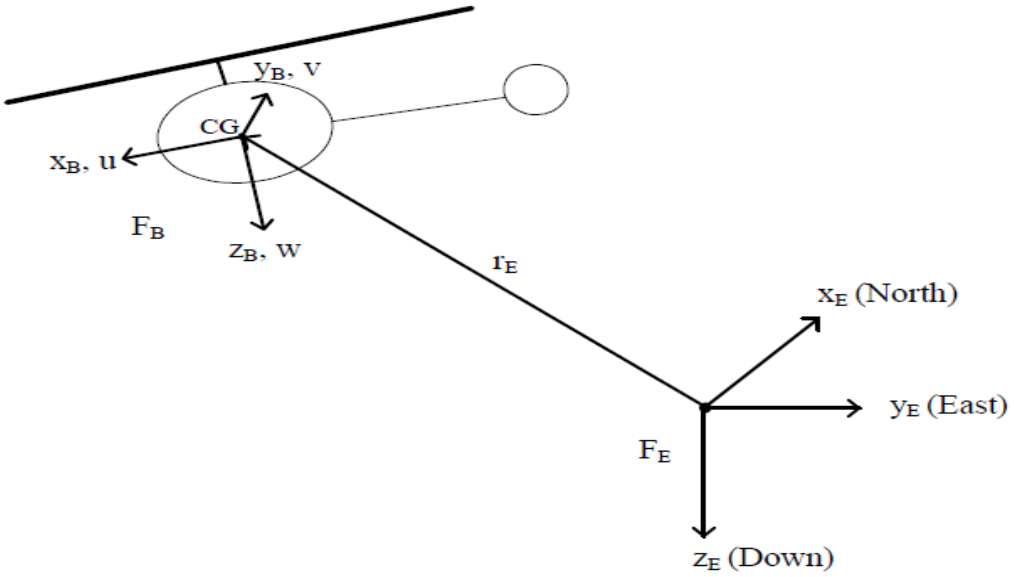

Figure 1.2: Body & earth frame of reference for helicopter
Source: Investigation of a non-uniform helicopter rotor downwash model by Berenike Hanson

1.4 Literature Review

Various methods have been proposed to develop control for helicopter stabilization. In [1] linear quadratic regulator based control was discussed. [2] suggested Lyapunov stability

based controller design. To reject external disturbances H_∞ based control is proposed in [3]. [4] and [5] applied model based tracking control for helicopters. [6] presented nonlinear back stepping control. This research work is based on rotational matrix utilization.

Many models and techniques have been presented to accurately capture dynamics of suspended payload with helicopter and stabilized payload. In [7] Dukes proposed dynamic suspension point instead of fixed one. This method is effective in reducing amplitude of vibrations however it is costly as compared to modification of control technique for system. [8] and [5] discussed model following control technique. [9] suggested payload state estimators but this technique require more computational time which decreases its applicability. [10] discussed vision based control to reject disturbances however its capability depend upon accurate measurement of load swing. Also due to utilization of image processing such method take longer time to apply corrective control input. Adams in [11] suggested input shapers for disturbance rejection but this method remain un effected on external disturbances. [12] used neural network based control for helicopters.

Rotor downwash modeling has been in terms of induced velocity. Momentum theory is proposed in [13] which utilize law of conservation of fluid mass, momentum and energy to derive relation for induced velocity. [14] used Blade Element Theory to derive relation for forces and moments of each blade. According to this theory each blade is decomposed into 2-D thin strips and each strip results in aerodynamic forces.

1.5 Contribution

It is evident from literature review that various strategies have been adapted to stabilize helicopter with attached payload by reducing effect of external disturbances. Techniques like input shaping are reliable in forcing payload to mean position but they are not capable of dealing with external disturbances. Other methods including visual based state estimators require more computation time which results in risk of system failure.

To cope up with all these issues sliding mode control could be a good solution. It is resilient to external disturbances moreover SMC offers fast response and has variable control structure. To make system robust characteristics of linear matrix inequality are utilized. LMI offers solution that is not optimum only at specific points but also globally most effective. Further LMIs provide easy problem formulation capability. All of these qualities make

combination of SMC and LMIs most suitable choice for developing control for payload stabilization.

1.5 Thesis Structure

This thesis work comprise of six chapters. The details of each chapter from chapter 2 are described below.

- **Chapter 1**

  Chapter 1 consists of motivation behind thesis topic selection, introduction to the topic and background of helicopters which include frame of references of helicopter, flight modes and types of helicopters on the basis of maneuvering and structure. It also covers literature review of the topic and contribution made in this thesis work.

- **Chapter 2**

  This chapter describes mathematical modeling of system. Modeling is done helicopter as well as payload. Two models of payload are presented in this thesis and analyses are performed on both of models separately. These models comprise of planar crane model which is allowed to move only in lateral direction while other model comprise of coupling between load and altitude. This model is allowed to move only in longitudinal direction. Moreover effects of rotor down wash in terms of induced velocity are also added to the payload model two.

- **Chapter 3**

  This chapter deals with control scheme utilized for helicopter stabilization. Sliding mode control based on linearized dynamics is described in this chapter. This part of research is based on work of Xian as proposed in [15]. This control technique is applied to system after dividing the model into two subsystems which include longitudinal-lateral subsystem as well as heading and heave subsystem. Separate control inputs are used for each subsystem.

- **Chapter 4**

  This chapter describes control development for payload subsystem. Two models of payload are presented in the research work. These models comprise of planar crane model which is allowed to move only in lateral direction while other model comprise

of coupling between load and altitude. This model is allowed to move only in longitudinal direction. Both of these models are analyzed separately.

- **Chapter 5**

  This chapter show and compare results on the basis of proposed and achieved trajectory.

- **Chapter 6**

  This chapter covers conclusion and possible future extension to this thesis work.

CHAPTER 2: SYSTEM MATHEMATICAL MODELING

2.1 Helicopter Mathematical Model

Helicopter model has been utilized as described by Xian in [15]. Figure 2.1 shows helicopter diagram. It is modeled in body frame of reference. System has 6 degree of freedoms which include roll, pitch and yaw movement as angular motion and linear motion along x, y and z axis respectively. This system is controlled by 4 control inputs which include longitudinal, lateral collective and cyclic control inputs. The details of these inputs are described in previous chapter.

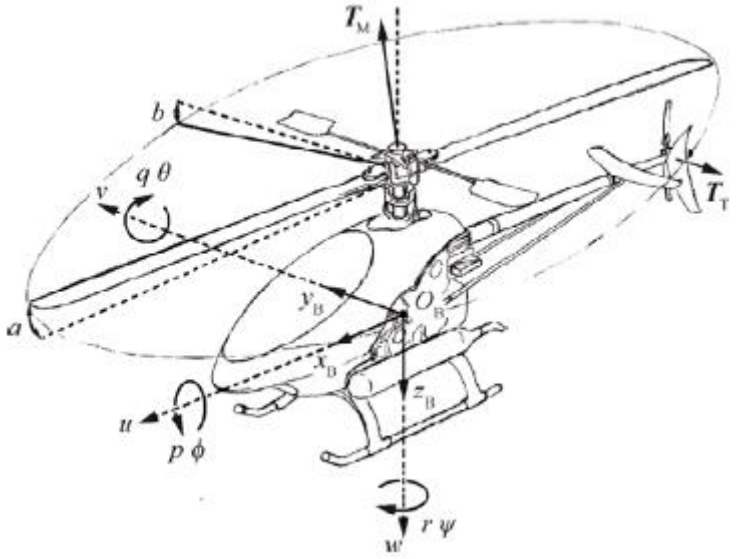

Figure 2.1: Helicopter in body fixed coordinate system
Source: Sliding mode tracking control for miniature unmanned helicopters by Xian Bin.

This under-actuated system has 11 states which include linear velocities along 3 axes represented as u, v and w respectively. p ,q and r represent angular velocities along x, y and z axes respectively. Φ, Θ and Ψ are roll, pitch and yaw angles respectively. a and b represent flapping angles along x and y axis. The model depicted in [15] is represented below.

$$m\dot{v}^B = -mS(\omega^B)v^B + mgR(\Theta)^T e_3 + T_M + d_{wind} \quad (2.1)$$

$$\dot{\Theta} = \psi(\Theta)\omega^B \quad (2.2)$$

$$J\dot{\omega}^B = -S(\omega^B)J\omega^B + M(T_{mr})v_c + N(T_{mr}) \quad (2.3)$$

$$\dot{a} = -q - \frac{1}{\zeta_f}a + A_b b + A_{lon}u_{lon} \quad (2.4)$$

$$\dot{b} = -p + B_a a - \frac{1}{\zeta_f} b + B_{lat} u_{lat} \quad (2.5)$$

$R(\Theta)$ describes orientation of body frame of reference w.r.t inertial frame of reference in terms of rotational matrix. $S(\omega^B)$ represents skew symmetric matric of angular velocity vector and $\psi(\Theta)$ angular velocity transfer matrix. Equation 2.2 depicts mapping of angular velocities from body frame of reference to blade frame of reference.

$$R(\Theta) = \begin{bmatrix} C(\Psi)C(\Theta) & -S(\Psi)C(\Phi) + C(\Psi)S(\Theta)S(\Phi) & S(\Phi)S(\Psi) + C(\Phi)S(\Theta)C(\Psi) \\ S(\Psi)C(\Theta) & C(\Phi)C(\Psi) + S(\Phi)S(\Theta)S(\Psi) & -C(\Psi)S(\Phi) + S(\Psi)S(\Theta)C(\Phi) \\ -S(\Theta) & C(\Theta)S(\Phi) & C(\Theta)C(\Phi) \end{bmatrix} \quad (2.6)$$

$$S(\omega^B) = \begin{bmatrix} 0 & -r & q \\ r & 0 & -p \\ -q & p & 0 \end{bmatrix} \quad (2.7)$$

$$\psi(\Theta) = \begin{bmatrix} 1 & S(\Phi)S(\Theta)/C(\Theta) & C(\Phi)S(\Theta)/C(\Theta) \\ 0 & C(\Phi) & -S(\Phi) \\ 0 & S(\Phi)/C(\Theta) & C(\Phi)/C(\Theta) \end{bmatrix} \quad (2.8)$$

$$T_M = [-T_{mr}a \quad T_{mr}b \quad -T_{mr}]^T \quad (2.9)$$

$$T_T = [0 \quad -T_{tr} \quad 0]^T \quad (2.10)$$

$$e_3 = [0 \quad 0 \quad 1]^T \quad (2.11)$$

$$d_w = [d_x \quad d_y \quad d_z]^T \quad (2.12)$$

$$v_c = [b \quad a \quad T_{tr}]^T \quad (2.13)$$

$$J = \begin{bmatrix} J_{xx} & 0 & 0 \\ 0 & J_{yy} & 0 \\ 0 & 0 & J_{zz} \end{bmatrix} \quad (2.14)$$

$$T_{mr} = K_m u_{col} + B_m \quad (2.15)$$

$$T_{tr} = K_t u_{ped} + B_t \quad (2.16)$$

T_M and T_T represent matrix thrust vector of main and tail rotor. e_3 is unit vector and d_w represent wind gust matrix. Value of v_c vector and inertia matric J is also shown above. ζ_f is main rotor time constant. T_{mr} and T_{tr} are magnitudes of main and tail rotor generated thrust respectively. A_{lon} and B_{lat} are input derivatives. K_m,K_t, B_m and B_t are thrust constants. A_b

and B_a represent rotor cross coupling effects. $M(T_{mr})$ account for invertible matrix for T_{mr} and $N(T_{mr})$ represent vector of parameters for T_{mr} ,values of these terms can be derived from [16].Using eq 2.6 to 2.16, equations 2.1-2.5 can be reduced to following with Table 2.1 depicts values of constants used in equations 2.17-2.27.

$$\dot{u} = vr - g\sin(\Theta) - wq - (A_a + A_b\, u_{col})a + A_x d_x \quad (2.17)$$

$$\dot{v} = g\cos(\Theta)\sin(\phi) - ur + wp + (A_a + A_b\, u_{col})b + A_x d_y \quad (2.18)$$

$$\dot{w} = g\cos(\phi)\cos(\Theta) + uq - vp - A_a - A_b\, u_{col} + A_x d_z \quad (2.19)$$

$$\dot{p} = p + (r\cos(\phi) + q\sin(\phi))\tan(\Theta) \quad (2.20)$$

$$\dot{q} = q\cos(\phi) - r\sin(\phi) \quad (2.21)$$

$$\dot{r} = (r\cos(\phi))/\cos(\Theta) + (q\sin(\phi))/\cos(\Theta) \quad (2.22)$$

$$\dot{\phi} = (A_e)qr + (A_h)b - (A_k)a - (A_m)u_{col}\, b - A_p\left(\sqrt[3]{A_c + A_d\, u_{col}}\right)a \quad (2.23)$$

$$\dot{\Theta} = (A_f)pr + (A_i)a + (A_l)b - (A_n)u_{col}\, a + A_q(\sqrt[3]{A_c + A_d\, u_{col}})b \quad (2.24)$$

$$\dot{\Psi} = (A_g)pq - (A_j) - (A_o)u_{ped} - A_r(\sqrt[3]{A_c + A_d\, u_{col}}) \quad (2.25)$$

$$\dot{a} = -q - (A_s)a + (A_v)b + (A_t)u_{lon} \quad (2.26)$$

$$\dot{b} = -p + (A_w)a - (A_s)b + (A_u)u_{lat} \quad (2.27)$$

Table 2.1 Constants of helicopter model

Sr No	**Constant Name**	**Value**
1.	A_a	11.0421
2.	A_b	10.0379
3.	A_c	104.9
4.	A_d	95.36
5.	A_e	-0.9522
6.	A_f	0.9781
7.	A_g	-0.3774
8.	A_h	595.2243
9.	A_i	272.6301
10.	A_j	-5.2683
11.	A_k	2.5116
12.	A_l	1.1504
13.	A_m	-128.0331

Sr No	Constant Name	Value
14.	A_n	-58.6429
15.	A_o	-30.3530
16.	A_p	0.0177
17.	A_q	0.0081
18.	A_r	0.0057
19.	A_s	3.3445
20.	A_t	2.575
21.	A_u	2.575
22.	A_v	2.233
23.	A_w	2.448
24.	A_x	0.1053

2.2 Payload Mathematical Model 1

Payload model is inspired by the fact that slung load dynamics is similar to dynamics of planar crane. Planar crane behaves similar to pendulum. The slung load model utilized here is proposed in [11]. It is 2 DOF model comprising of helicopter displacement in lateral direction (y) and payload deflection angle (α). Figure 2.2 shows payload model.

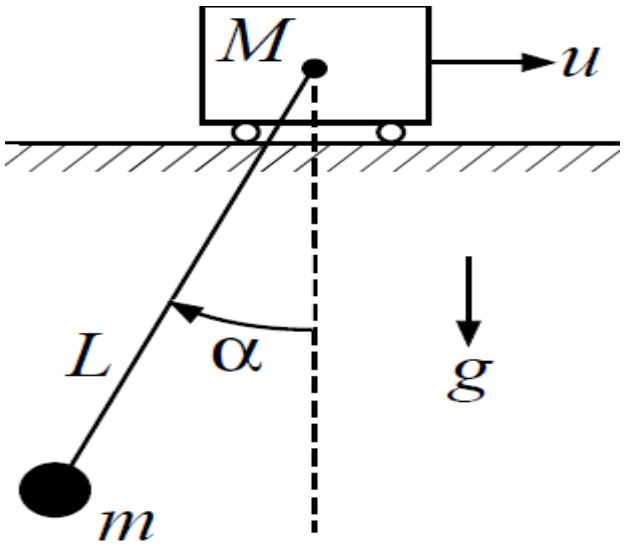

Figure 2.2: Payload model
Source: Modeling and control of helicopters carrying suspended loads by Christopher James Adams

The nonlinear model of payload is described as eq 2.28 and 2.29. m is mass of payload while M accounts for mass of helicopter. D_P and D_H represent damping coefficients for payload angle and helicopter position. These parameters account for aerodynamic drag. L is length of suspended payload cable. This model is analyzed by considering helicopter stationary in longitudinal direction, also heading and height of helicopter remain constant. Helicopter is only allowed to move in lateral direction. Payload is assumed to be attached at helicopter center of gravity.

$$\ddot{y} = \frac{-m\sin(\alpha)(L\dot{\alpha}^2+g\cos(\alpha))}{M+m\sin^2(\alpha)} + \frac{1}{M+m\sin^2(\alpha)}u - \frac{D_H}{M}\dot{y} \quad (2.28)$$

$$\ddot{\alpha} = \frac{-(m+M)g\sin(\alpha)-mL\dot{\alpha}^2\sin(\alpha)\cos(\alpha)}{ML+mL\sin^2(\alpha)} + \frac{\cos(\alpha)}{ML+mL\sin^2(\alpha)}u - \frac{D_P}{m}\dot{\alpha} \quad (2.29)$$

Table 2.2 Payload subsystem constants

Sr No	**Constant Name**	**Value**
1.	M	9.5 kg
2.	m	0.5 kg
3.	L	1.5 m
4.	D_H	0.8
5.	D_P	0.5

2.3 Payload Mathematical Model 2

When previous is model is tested on practical systems and conclusions were drawn, it was observed that real flight data differs from simulated results in case of lateral translation. From experimental verification it is evident that previous model has some short comings. To make the model more realistic load altitude coupling is incorporated in model. This coupling will model relation between payload and roll altitude.

Load altitude coupling model incorporates distance between suspension point of slung load cable to helicopter and helicopter center of gravity. So this model is more realistic since in real helicopters load is not attached to COG of helicopter. In this model helicopter is assumed

to be stationary in lateral direction. Its motion is only allowed in longitudinal direction. Figure 2.3 shows system's degree of freedom of new payload subsystem.

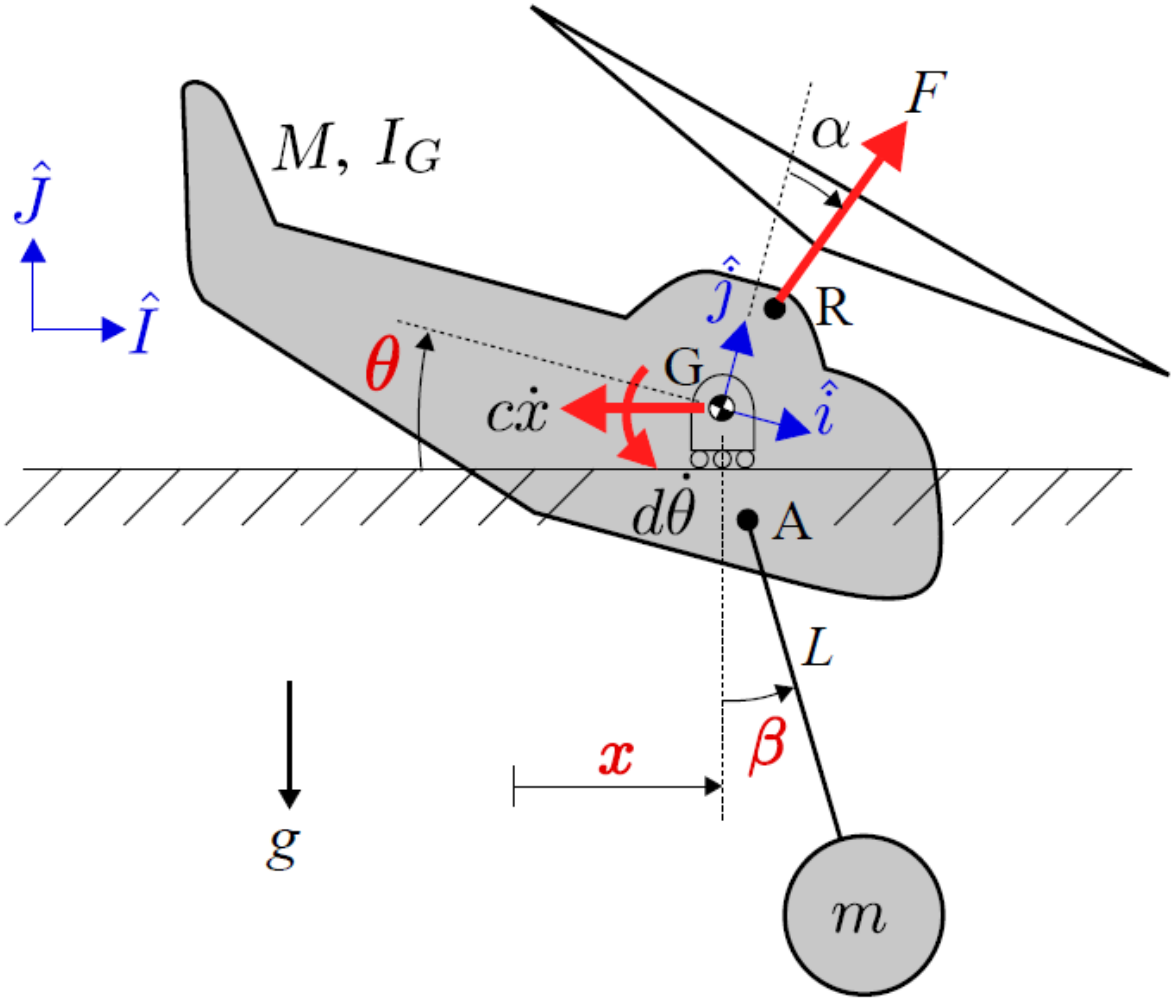

Figure 2.3: Payload model 2 pictorial view
Source: Modeling and control of helicopters carrying suspended loads
by Christopher James Adams

Helicopter is allowed to rotate about center of gravity of helicopter G. Helicopter maintains constant height from ground and its direction also remain unchanged. L is length of cable which is assumed to be weightless and rigid. m is mass of payload and it is assumed to be point mass. Aerodynamic drag is also part of model as dampers with damping coefficient as c. Θ is pitch angle of helicopter. β represents angle of deflection of payload with respect to vertical direction. M is mass of helicopter. I_G represents moment of inertia of helicopter. d is coefficient of rotational damper for helicopter altitude. α is angle of longitudinal tilting for rotor. F is assumed to be generated thrust of main thrust.

Rotor is assumed to be quasi-static so that rotor can be tilted instantaneously with cyclic control input. Lagrange's method is used to derive system of equations. Complete derivation of equations can be accessed from [17]. The nonlinear equations of this payload subsystem are shown as equations 2.30 to 2.32.

$$(M+m)\ddot{x} + mL\ddot{\beta}\cos(\beta) - m(x_A\sin(\Theta) - y_A\cos(\Theta))\ddot{\Theta} + c\dot{x} - mL\dot{\beta}^2\sin(\beta) + m(x_A\cos(\Theta) + y_A\sin(\Theta))\dot{\Theta}^2 = F\sin(\alpha+\Theta) \quad (2.30)$$

$$\left(I_G + m({x_A}^2 + {y_A}^2)\right)\ddot{\Theta} + d\dot{\Theta} - m(x_A\sin(\Theta) - y_A\cos(\Theta))\ddot{x} - gm(x_A\cos(\Theta) + y_A\sin(\Theta)) - mL(x_A\sin(\Theta+\beta) - y_A\cos(\Theta+\beta))\ddot{\beta} - mL(x_A\cos(\Theta+\beta) + y_A\sin(\Theta+\beta))\dot{\beta}^2 = F(y_R\sin(\alpha) - x_R\cos(\alpha)) \quad (2.31)$$

$$L\ddot{\beta} + \ddot{x}\cos(\beta) - (x_A\sin(\Theta+\beta) - y_A\cos(\Theta+\beta))\ddot{\Theta} - (x_A\cos(\Theta+\beta) + y_A\sin(\Theta+\beta))\dot{\Theta}^2 + g\sin(\beta) = 0 \quad (2.32)$$

x_A and y_A represent horizontal and vertical distance respectively between helicopter COG and point of suspension while x_R and y_R are distance parameters for distance between point R and COG of helicopter as shown in Figure 2.3. Both of payload models are analyzed separately during this research work and their results are shown in next chapters.

2.4 External Disturbance Model

External disturbances (wind gusts) are assumed to be sinusoidal wave with some amplitude. These disturbances are assumed to be time varying. This type of disturbance is used by [15] and [18]. Following is sample of disturbances that is used for modeling air disturbances.

Table 2.3. Air disturbances

Time $(t)_{sec}$	**d_x**	**d_y**	**d_z**
$t \leq 15$	$0.1\sin(\pi t)$	$0.1\sin(\pi t)$	0
$15 < t \leq 30$	$0.1\sin(\pi t)$	0	0
$30 < t \leq 45$	0	$0.1\sin(\pi t)$	0
$45 < t \leq 60$	0	0	$0.1\sin(\pi t)$
$t \geq 60$	0	0	0

2.5 Rotor Downwash Model (Hovering)

The rotor downwash model is inspired by work in [13] and [14]. In case of helicopters flow field is much complex than of aero-planes. Aero-planes vortices at tip trail downward immediately while in case of helicopters tip vortices remain in vicinity of rotor for longer interval of time. These tip vortices result in induced velocity while cause variable air loads on rotor; resulting in inducing vibrations in rotor and system. Figure 2.4 shows velocity distribution field.

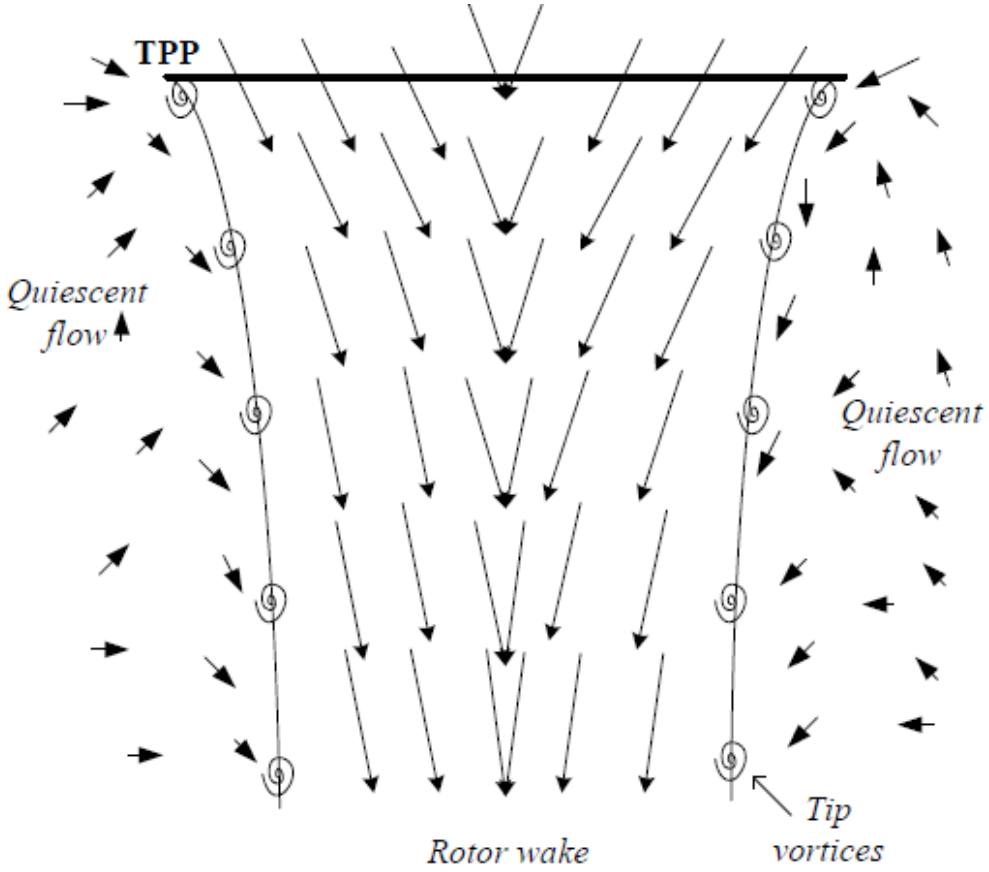

Figure 2.4: Velocity flow field
Source: Investigation of a non-uniform helicopter rotor downwash model by Berenike Hanson

In this thesis momentum theory is utilized to derive relation for induced velocity. It is based upon conservation of three laws.

- Law of conservation of fluid mass
- Law of conversation of energy
- Law of conservation of fluid momentum

This theory provides separate relations for hovering as well as forward flight. Only relation for hovering is utilized. Uniform inflow model is used in system equations development. Figure 2.5 shows various inflow models.

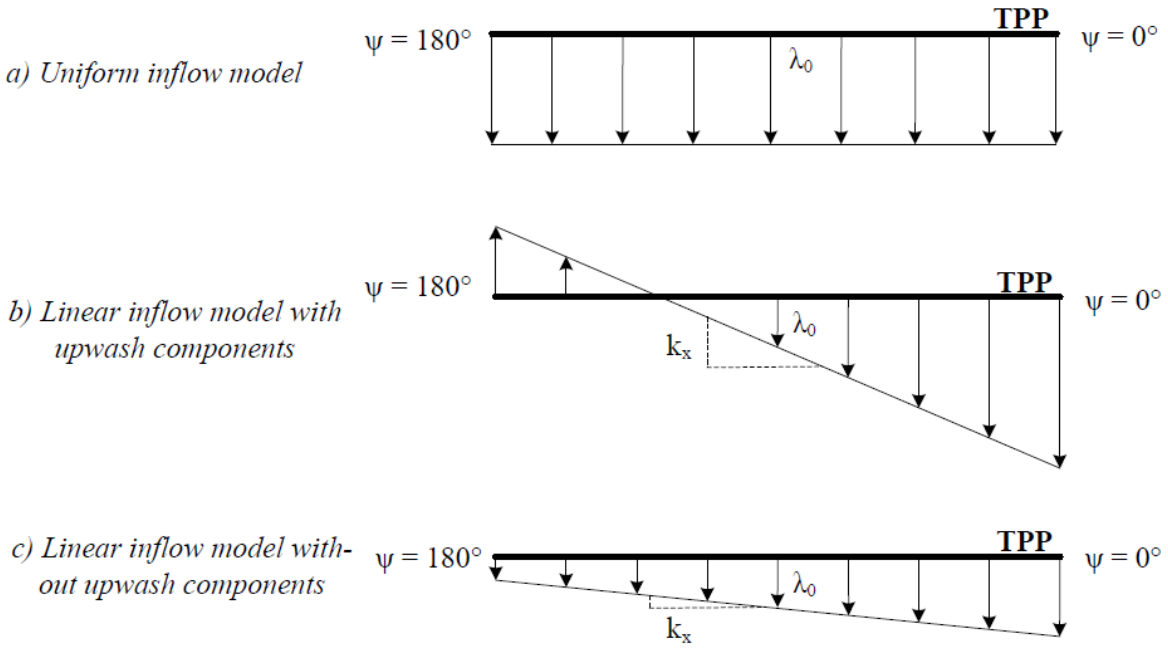

Figure 2.5: Types of inflow models
Source: Investigation of a non-uniform helicopter rotor downwash model by Berenike Hanson

It is assumed that inflow passing through rotor is incompressible, in-viscid, almost steady (flow properties does not vary with time) and is uniform over whole disk formed by rotor during rotation. Let A denotes area of rotor disk. Assume that volume in vicinity of rotor including produced wake has surface area denoted by S. Induce velocity magnitude increases as soon as wake area decreases while traveling downward. It is further assumed that volume comprising rotor and produced wake is divided into various planes with plane zero lies at far distance above rotor itself. Plane infinity is located downward in far wake. Figure 2.6 shows division of this whole volume in different planes where dS denotes unit vector normal to whole control volume. According to law of conservation of fluid mass, mass flow rate must be constant with in whole volume. This statement is supported by expression of the law which is shown as following;

$$\iint_S \rho V.\, dS = 0 \qquad (2.33)$$

where ρ is density of air, while V represents velocity of air flowing downward in near locality.

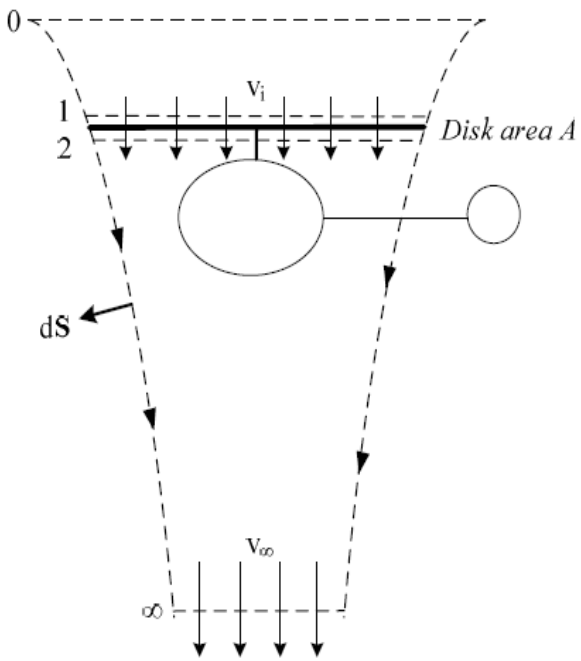

Figure 2.6: Control volume comprising wake and rotor surrounding
Source: Investigation of a non-uniform helicopter rotor downwash model by Berenike Hanson

Since flow is assumed to be quasi-steady so law of conservation of mass can be expressed in terms of following expression with A_∞ and v_∞ represent area of wake and velocity at far below disk of rotor, A_2 is area of plane below disk while v_i represents induce velocity at disk of rotor.

$$\dot{m} = \rho A_\infty v_\infty = \rho A_2 v_i = \rho A v_i \tag{2.34}$$

Equation (2.35) represents law of fluid momentum conservation. Since this air inflow is unconstrained, so the net pressure p on it inside whole control volume will be zero. Now only force which exert on liquid is equal to rate of change fluid momentum with respect to time. This force F_f is equal in magnitude but opposite in direction to thrust of main rotor. Equations (2.36) to (2.38) comprise these relations. Last term in (2.36) can be reduced to zero since flow properties remain constant even far above disk of main rotor. Eq (2.37) gives relation of thrust of main rotor.

$$F_f = \iint_S pdS + \iint_S (\rho V.\, dS)V \tag{2.35}$$

$$-F_f = T_{mr} = \iint_\infty (\rho V.\, dS)V - \iint_0 (\rho V.\, dS)V \tag{2.36}$$

$$T_{mr} = \iint_\infty (\rho V.\, dS)V = \dot{m} v_\infty \tag{2.37}$$

By definition of law of conservation of energy work done by main rotor on inflow results in gain in kinetic energy with respect to time in slipstream of rotor. In case of main rotor work done per unit time is expressed as (2.39) which can be reduced to (2.40) by assuming flow is quiescent above rotor.

$$W = \iint_S 0.5(\rho V.\, dS)|V|^2 \tag{2.38}$$

$$T_{mr} v_i = \iint_\infty 0.5(\rho V.\, dS)V^2 - \iint_0 0.5(\rho V.\, dS)V^2 \tag{2.39}$$

$$T_{mr} v_i = \iint_\infty 0.5(\rho V.\, dS)V^2 = 0.5\, \dot{m} {v_\infty}^2 \tag{2.40}$$

Using above used relations (2.41) can be derived, which can be used to update equation of main rotor thrust. Now after rearranging eq (2.43) relation for velocity during hovering can be easily derived. This relation is expressed as (2.43).

$$v_\infty = 2\, v_i \tag{2.41}$$

$$T_{mr} = \dot{m} v_\infty = \dot{m} 2 v_i = \rho A v_i 2 v_i = 2\rho A {v_i}^2 \tag{2.42}$$

$$v_h = v_i = \sqrt{\frac{T_{mr}}{2\rho A}} \tag{2.43}$$

Thrust coefficient C_T equation is described as (2.44). It is a non-dimensional quantity. With the help of (2.43) and (2.44) value of induced inflow in terms of thrust coefficient can be easily derived. Equation (2.45) is valid for uniformly distributed inflow.

$$C_T = \frac{T_{mr}}{\rho A \Omega^2 R^2} \tag{2.44}$$

$$\lambda_h = \lambda_i = \frac{v_i}{\Omega R} = \frac{1}{\Omega R}\sqrt{\frac{T_{mr}}{2\rho A}} = \sqrt{\frac{C_T}{2}} \tag{2.45}$$

CHAPTER 3: CONTROL SCHEME FOR HELICOPTER

This control scheme utilized here is inspired by the work of Xian [15]. This work is based on sliding mode control based on linearized dynamics. Separate controls are developed longitudinal-lateral subsystem and heading–heave system.

3.1 Longitudinal-Lateral Subsystem

This subsystem consists of 8 states which are listed below as (3.1) and 2 control inputs listed as (3.2). This system is clearly under-actuated as depicted by (3.1) and (3.2). External disturbances are added in longitudinal as well as lateral direction, its vector form is shown in (3.3).

$$\mathbf{x} = (u \;\; v \;\; \theta \;\; \phi \;\; q \;\; p \;\; a \;\; b) \tag{3.1}$$

$$\mathbf{u} = (u_{long} \;\; u_{lat}) \tag{3.2}$$

$$\mathbf{d} = (d_x \; d_y) \tag{3.3}$$

The linearized subsystem is depicted as (3.4) to (3.11). The longitudinal-lateral subsystem part of equations (2.1) to (2.5) is slightly non-minimal but translational forces generated by main rotor flapping motion are negligibly small so they are assumed to be external perturbations.

$$\dot{u} = X_u u - g\theta + d_x \tag{3.4}$$

$$\dot{v} = Y_v v + g\phi + d_y \tag{3.5}$$

$$\dot{q} = M_u u + M_v v + M_a a \tag{3.6}$$

$$\dot{p} = L_u u + L_v v + L_b b \tag{3.7}$$

$$\dot{\theta} = q \tag{3.8}$$

$$\dot{\phi} = p \tag{3.9}$$

$$\dot{a} = -q - \frac{1}{\zeta_f} a + A_b b + A_{lon} u_{lon} \tag{3.10}$$

$$\dot{b} = -p + B_a a - \frac{1}{\zeta_f} b + B_{lat} u_{lat} \tag{3.11}$$

In order to track pre-defined velocities, tracking error is defined for longitudinal and lateral velocities as (3.12).

$$e_1 = \begin{bmatrix} e_u \\ e_v \end{bmatrix} = \begin{bmatrix} u \\ v \end{bmatrix} - \begin{bmatrix} u_{ref} \\ v_{ref} \end{bmatrix} \tag{3.12}$$

After taking time derivative of above equation and then adding and subtracting $[X_u u_r \quad Y_v v_r]^T$ we get following expression.

$$\dot{e_1} = \begin{bmatrix} \dot{e_u} \\ \dot{e_v} \end{bmatrix} = \begin{bmatrix} \dot{u} \\ \dot{v} \end{bmatrix} - \begin{bmatrix} \dot{u_{ref}} \\ \dot{v_{ref}} \end{bmatrix} + \begin{bmatrix} X_u u_r \\ Y_v v_r \end{bmatrix} - \begin{bmatrix} X_u u_r \\ Y_v v_r \end{bmatrix} \tag{3.13}$$

Putting value of (3.4) and (3.5) in above equation and simplifying we obtain (3.14) with $K_1 = \text{diag}(X_u, Y_v)$, $K_2 = \text{diag}(-g, g)$. Value of N_d is shown as (3.15).

$$e_2 = K_1 e_1 + K_2 \begin{bmatrix} \theta \\ \phi \end{bmatrix} + N_d \tag{3.14}$$

$$N_d = K_1 \begin{bmatrix} u_{ref} \\ v_{ref} \end{bmatrix} - \begin{bmatrix} \dot{u_{ref}} \\ \dot{v_{ref}} \end{bmatrix} + \begin{bmatrix} d_1 \\ d_2 \end{bmatrix} \tag{3.15}$$

Taking time derivative of (3.14) and putting value of (3.4) to (3.11) which ever valid in resulting expression and simplifying we get (3.16)

$$e_3 = K_1 e_2 + K_2 \begin{bmatrix} q \\ p \end{bmatrix} + \dot{N_d} \tag{3.16}$$

Once again applying same process as with (3.14) we get following results

$$e_4 = K_1 e_3 + K_2 \begin{bmatrix} M_u u + M_v v + M_a a \\ L_u u + L_v v + L_a a \end{bmatrix} + \ddot{N_d} \tag{3.17}$$

For controller designing we selected following sliding surface with $Л = [\lambda_1 \ \ \lambda_2]^T$ is control gain matrix.

$$s = \begin{bmatrix} s_1 \\ s_2 \end{bmatrix} = e_4 + 3Лe_3 + 3Л^2 e_2 + Л^3 e_1 \tag{3.18}$$

$e_1$can be imagined to obtained from s via 3rd order low pass filter with time constants ${\lambda_1}^{-1}$ and ${\lambda_2}^{-1}$. $e_1$will have same steady characters as of s due to property of linear systems. By taking derivative of s and putting value of (3.4) to (3.11) which ever valid and utilizing (3.14), (3.16) and (3.17) in resulting expression we get following relation.

$$\dot{s} = D_1 + h_1 + K_2 K_3 K_4 \begin{bmatrix} u_{long} \\ u_{lat} \end{bmatrix} \tag{3.19}$$

With $K_3 = \mathrm{diag}(M_a, L_b)$ and $K_4 = \mathrm{diag}(A_{lon}, B_{lat})$ and auxiliary function $h_1$and D_1 are defined as following

$$D_1 = K_2 K_3 \begin{bmatrix} -\frac{1}{\zeta_f} a + A_b b \\ B_a a - \frac{1}{\zeta_f} b \end{bmatrix} + \ddot{N}_d \tag{3.20}$$

$$h_1 = K_1 e_4 + K_2 \begin{bmatrix} M_u(X_u u - g\theta) + M_v(Y_v v + g\phi) \\ L_u(X_u u - g\theta) + L_v(Y_v v + g\phi) \end{bmatrix} - K_2 K_3 \begin{bmatrix} q \\ p \end{bmatrix} + 3Л e_4 + 3Л^2 e_3 Л^3 e_2 \tag{3.21}$$

Using (3.19) controller is designed as following. $\beta_1$and β_2 are control gains.

$$\begin{bmatrix} u_{long} \\ u_{lat} \end{bmatrix} = (K_2 K_3 K_4)^{-1} \left(-h_1 - \begin{bmatrix} \beta_1 \mathrm{sgn}(s_1) \\ \beta_2 \mathrm{sgn}(s_2) \end{bmatrix} - \begin{bmatrix} k_1 s_1 \\ k_2 s_2 \end{bmatrix} \right) \tag{3.22}$$

Putting value of control inputs obtained above into (3.19) we get following simplified version of (3.19).

$$\dot{s} = D_1 - \begin{bmatrix} \beta_1 \mathrm{sgn}(s_1) \\ \beta_2 \mathrm{sgn}(s_2) \end{bmatrix} - \begin{bmatrix} k_1 s_1 \\ k_2 s_2 \end{bmatrix} \tag{3.23}$$

Control inputs as in (3.22) ensures global exponential convergence of tracking error of longitudinal and lateral velocities as depicted following when selected $\beta_1$and β_2 holds (3.25).

$$\lim_{t \to \infty} e_1 = 0 \tag{3.24}$$

$$\begin{Bmatrix} \boldsymbol{\beta_1} \geq \| [\mathbf{1} \quad \mathbf{0}] \mathbf{D_1} \| \\ \boldsymbol{\beta_2} \geq \| [\mathbf{1} \quad \mathbf{0}] \mathbf{D_2} \| \end{Bmatrix} \tag{3.25}$$

Lyapunov function is selected as following

$$V_1 = \frac{1}{2} s^T s \tag{3.26}$$

Taking time derivation of above expression and simplifying with the help of (3.23) we get.

$$\dot{V}_1 = s^T D_1 - \beta_1 |s_1| - \beta_2 |s_2| - k_1 {s_1}^2 - k_2 {s_2}^2$$

Due to (3.25) following result can be drawn, where $k_{min} = \min[k_1, k_2]$

$$\dot{V}_1 \leq -k_{min} s^T s = -2 k_{min} V_1$$

It can be easily seen that Lyapunov function also converges since it is non-negative function.

3.2 Heading-Heave Subsystem

This subsystem consists of 3 states which are listed below as (3.27) and 2 control inputs listed as (3.28). External disturbances are added in vertical direction, its vector form is shown in (3.29). The linearized subsystem is depicted as (3.30) to (3.32).

$$\mathbf{x} = (\Psi \;\; r \;\; w) \tag{3.27}$$

$$\mathbf{u}= (u_{ped} \;\; u_{col}) \tag{3.28}$$

$$\mathbf{d} = (d_z) \tag{3.29}$$

$$\dot{\Psi} = r \tag{3.30}$$

$$\dot{r} = N_v v + N_p p + N_w w + N_r r + N_{ped} u_{ped} \tag{3.31}$$

$$\dot{w} = Z_a a + Z_b b + Z_w w + Z_r r + d_3 + Z_{col} u_{col} \tag{3.32}$$

3.2.1 Heading Dynamics

Yaw angle tracking error can be defined as (3.33) and sliding surface is designed as (3.34). λ_3 represents control gain. Integral of error in (3.34) can be assumed to be obtained from sliding surface s via 2nd order low pass filter. Taking time derivative of (3.34) and simplifying with the help of (3.30) to (3.32) we get (3.35).

$$e_\Psi = \Psi - \Psi_{ref} \tag{3.33}$$

$$s = \left(\frac{d}{dt} + \lambda_3\right)^2 \int_0^t e_\Psi(\zeta) d\zeta \tag{3.34}$$

$$\dot{s} = D_2 + h_2 + N_{ped} u_{ped} \tag{3.35}$$

Values of auxiliary functions D_2 and h_2 are described as (3.36) and (3.37).

$$D_2 = -\ddot{\Psi}_{ref} - 2\lambda_3 \dot{\Psi}_{ref} \tag{3.36}$$

$$h_2 = N_v v + N_p p + N_w w + N_r r + 2\lambda_3 r + {\lambda_3}^2 e_\Psi \tag{3.37}$$

Using (3.35) control input u_{ped} is selected as following.

$$u_{ped} = \frac{1}{N_{ped}}(-h_2 - \beta_3 sgn(s) - k_3 s) \quad (3.38)$$

$$\dot{s} = D_2 - \beta_3 sgn(s) - k_3 s \quad (3.39)$$

A control input as in (3.38) ensures global exponential convergence of tracking error as depicted following when selected β_3 (3.41).

$$\lim_{t\to\infty} e_\Psi = 0 \quad (3.40)$$

$$\beta_3 \geq \|D_2\|_\infty \quad (3.41)$$

Lyapunov function is selected as following

$$V_2 = \frac{1}{2}s^2 \quad (3.42)$$

Taking time derivation of above expression and simplifying with the help of (3.39) we get.

$$\dot{V}_2 = sD_2 - \beta_3|s| - \beta_2|s| - k_3 s^2 \quad (3.43)$$

Due to (3.41) and (3.43) following result can be drawn,

$$\dot{V}_2 \leq -k_3 s^2 = -2k_3 V_2 \quad (3.44)$$

3.2.2 Heave Dynamics

Error for vertical velocity tracking is utilized in such dynamics as depicted below

$$e_w = w - w_{ref} \quad (3.45)$$

Taking derivation of above expression we get

$$\dot{e_w} = D_3 + h_3 + Z_{col} u_{col} \quad (3.46)$$

Values of auxiliary functions D_3 and h_3 are described as (3.47) and (3.48).

$$D_3 = Z_a a + Z_b b - \dot{w_{ref}} + d_3 \quad (3.47)$$

$$h_3 = Z_w w + Z_r r \quad (3.48)$$

Using (3.46) control input u_{col} is selected as following.

$$u_{col} = \frac{1}{Z_{col}}(-h_3 - \beta_4 sgn(e_w) - k_i \int_0^t e_w(\zeta)d\zeta - k_p e_w) \quad (3.49)$$

$$\dot{e_w} = D_3 - \beta_4 sgn(e_w) - k_i \int_0^t e_w(\zeta)d\zeta - k_p e_w \quad (3.50)$$

β_4, k_i and k_p represent selected control gains. A control input as in (3.49) ensures global exponential convergence of tracking error as depicted following when selected β_4 (3.52).

$$\lim_{t\to\infty} e_w = 0 \quad (3.51)$$

$$\beta_4 \geq \|D_3\|_\infty \quad (3.52)$$

Lyapunov function is selected as following

$$V_3 = \frac{1}{2} e_w{}^2 + \frac{k_i}{2} \left(\int_0^t e_w(\zeta)d\zeta\right)^2 \quad (3.53)$$

Taking time derivation of above expression and simplifying with the help of (3.46) we get.

$$\dot{V_3} = e_w D_3 - \beta_4 |e_w| - k_p e_w{}^2 \quad (3.54)$$

Due to (3.52) and (3.54) following result can be drawn,

$$\dot{V_3} \leq -k_p e_w{}^2 \quad (3.55)$$

CHAPTER 4: CONTROL SCHEME FOR PAYLOAD

Both payload models are stabilized on the basis of proposed control scheme. Linear Matrix Inequity based Sliding Mode Control (SMC) is used. Such control system is used by [18] and [19]. Both systems are linearized about hovering condition and developed control applied on both systems separately. The linearized systems are shown below.

4.1 Linearized Payload Model 1

Equations (2.28) and (2.29) are linearized for hovering condition. Linearized system is represented as following state space matrix and noise in lateral direction is also added to system.

$$\begin{bmatrix} \dot{\alpha} \\ \ddot{\alpha} \\ \dot{y} \\ \ddot{y} \end{bmatrix} = \begin{bmatrix} 0 & 1 & 0 & 0 \\ f_1 & f_2 & 0 & 0 \\ 0 & 0 & 0 & 1 \\ f_3 & 0 & 0 & f_4 \end{bmatrix} + \begin{bmatrix} 0 \\ f_5 \\ 0 \\ f_6 \end{bmatrix} (u + d_y(t)) \tag{4.1}$$

u is control input which represent lateral control input on system. Constants in (4.1) are represented as following Table 4.1

Table 4.1 Linearized payload model 1

Sr No	Constant Name	Value
1.	f_1	$-\frac{g(M+m)}{ML}$
2.	f_2	$-\frac{D_P}{m}$
3.	f_3	$-\frac{mg}{M}$
4.	f_4	$-\frac{D_H}{M}$
5.	f_5	$\frac{1}{ML}$
6.	f_6	$\frac{1}{M}$

Above system is analyzed by keeping the payload stationary in longitudinal direction and allowing payload motion in lateral direction. Objective of control scheme is to force payload

deflection angle as well its angular rate to zero and keeping the helicopter stationary in lateral direction. For this purpose control scheme is developed.

4.2 Linearized Payload Model 2

Equations (2.30) to (2.32) are linearized after adding induced velocity effect to system and changing sign conventions according to body frame of reference. Payload is allowed to move only in longitudinal direction while motion of payload is restricted in lateral direction. Equation (4.2) represents linearized system according to hovering conditions and noise in longitudinal direction is also added to system.

$$\begin{bmatrix} \dot{x} \\ \ddot{x} \\ \dot{\theta} \\ \ddot{\theta} \\ \dot{\alpha} \\ \ddot{\alpha} \end{bmatrix} = \begin{bmatrix} 0 & 1 & 0 & 0 & 0 & 0 \\ 0 & c_1 & c_2 & 0 & c_3 & 0 \\ 0 & 0 & 0 & 1 & 0 & 0 \\ 0 & 0 & c_4 & c_5 & c_6 & 0 \\ 0 & 0 & 0 & 0 & 0 & 1 \\ 0 & c_7 & c_8 & c_9 & c_{10} & 0 \end{bmatrix} \begin{bmatrix} x \\ \dot{x} \\ \theta \\ \dot{\theta} \\ \alpha \\ \dot{\alpha} \end{bmatrix} + \begin{bmatrix} 0 \\ c_{11} \\ 0 \\ c_{12} \\ 0 \\ c_{13} \end{bmatrix} (u_\beta + d_x(t)) \qquad (4.2)$$

Constants used in above state space matrix are listed as Table 4.2.

Table 4.2 Linearized payload model 2

Constant	Value
c_1	$-\,c\,L\,I_g$
c_2	$-\,F\,L\,I_g$
c_3	$-\,m\,L\,I_g\,(g+v_i)$
c_4	$-\,m\,L\,M\,y_a\,(g+v_i)$
c_5	$-M\,L\,d$
c_6	$-\,m\,L\,M\,y_a\,(g+v_i)$
c_7	$c\,I_g$
c_8	$F\,I_g + m\,M\,y_a{}^2\,(g+v_i)$
c_9	$M\,d\,y_a$
c_{10}	$(g+v_i)\,(I_g\,(m+M) + m\,M\,y_a{}^2)$
c_{11}	$-L\,F\,I_g$
c_{12}	$-L\,F\,M\,y_r$

c_{13}	$F\ (I_g + My_a y_r)$

v_i represents induce velocity. u_β represents tilt angle of main rotor control input. This input is used to control longitudinal motion of helicopter due to quasi-static representation of rotor.

4.3 Proposed Control Scheme

In this proposed technique model can track desired trajectory by keeping system states on sliding surface (s). Two types of inputs are used in this proposed controller.

- Nominal control input
- Equivalent control input

Nominal control input is used for forcing states of system on surface of sliding (s). In other words if states are far away from s this input ensures its return back to sliding surface. Equivalent control input is responsible for keeping states on this surface once nominal input results in delivering states on sliding surface. Selected sliding surface is shown as equation (4.3).

$$s = B^T L x \tag{4.3}$$

In above equation L is symmetric positive define matrix of size n x n, where n is number of states of system and x represents vector of states. Control input with details is shown below as following.

$$u_{in} = u_n + u_e \tag{4.4}$$

$$u_n = -(B^T L B)^{-1}(|B^T L B|\zeta_{max} + \varepsilon_0)\ \mathrm{sgn}(s) \tag{4.5}$$

$$u_e = -(B^T L B)^{-1} B^T L A x \tag{4.6}$$

In equation (4.5) ζ_{max} is max value or upper bound of disturbance. The mathematical expression for ζ_{max} is shown as equation (4.7). ε_0 is constant chosen to be greater than zero ($\varepsilon_0 > 0$).

$$|d(t)| \leq \zeta_{max} \tag{4.7}$$

where d(t) is disturbance is selected direction (the direction in which payload is allowed to move freely). Lyapunov function (V) is selected as (4.8).

$$V = \frac{1}{2}s^2 \tag{4.8}$$

Taking the derivative of sliding surface s and simplifying in following steps we get result which is shown as in (4.12) and (4.13).

$$\dot{s} = B^T L\dot{x} \tag{4.9}$$

$$\dot{s} = B^T L(Ax + B(u_{in} + d(t))) \tag{4.10}$$

$$\dot{s} = B^T LAx + B^T LBu_{in} + B^T LBd(t) \tag{4.11}$$

Putting value of u_{in} in (4.11) and simplifying we get the following expression. Considering few terms of (4.12) as (4.13).

$$\dot{s} = B^T LAx + B^T LB(-(B^T LB)^{-1}(|B^T LB|\zeta_{max} + \varepsilon_0)\, sgn(s) - (B^T LB)^{-1}B^T LAx) + B^T LBd(t) \tag{4.12}$$

$$\dot{s} = -(|B^T LB|\zeta_{max} + \varepsilon_0)\, sgn(s) + B^T LBd(t) \tag{4.13}$$

Taking time derivative of (4.8) we get (4.14). Putting values of s and $\dot{s}$ in it, we obtain (4.15). From (4.15) it is evident that condition (4.16) holds.

$$\dot{V} = s\dot{s} \tag{4.14}$$

$$\dot{V} = -(|B^T LB|\zeta_{max} + \varepsilon_0)\, |s| + B^T LBd(t) \tag{4.15}$$

$$\dot{V} \leq -\varepsilon_0\, |s| \tag{4.16}$$

To attain value of matrix L controller is developed as depicted below. Such method is proposed by [20]. Control input is selected as (4.17). Value of g(t) is shown as (4.18), so in this way controller input is amended.

$$u_{in}(t) = -Jx + g(t) \tag{4.17}$$

$$g(t) = Jx + u_n + u_e \tag{4.18}$$

J is vector of rank 1 x n exist such that modified matrix $\bar{A} = A - BJ$ remains stable for value of J. So modified system can be represented as (4.19). Matrix $\bar{A}$ has same rank as of A.

$$\dot{x}(t) = \bar{A}x + B\big(g + d(t)\big) \tag{4.19}$$

New Lyapunov function is selected as (4.20). Time derivative of (4.20) results are shown as (4.21) to (4.23).

$$V = x^{T}Lx \tag{4.20}$$

$$\dot{V} = 2x^{T}L\dot{x} \tag{4.21}$$

$$\dot{V} = 2x^{T}L(\bar{A}x(t) + B\big(g + d(t)\big)) \tag{4.22}$$

$$\dot{V} = 2x^{T}L\bar{A}x(t) + 2x^{T}LB(g + d(t)) \tag{4.23}$$

At $t \geq t_o$ $s = B^{T}Lx$ and $s^{T} = x^{T}LB$ become zero. So (4.23) can further modified as following with $M = L\bar{A} + \bar{A}^{T}L$.

$$\dot{V} = 2x^{T}L\bar{A}x(t) \tag{4.24}$$

$$\dot{V} = x^{T}(L\bar{A} + \bar{A}^{T}L)x \tag{4.25}$$

For obtaining $\dot{V} < 0$, M < 0 is needed to be satisfied. Lyapunov Stability Theorem is utilized to prove stability of system. According to this theorem $\bar{A}$ would be Hurwitz only if all eigen values of $\bar{A}$ have negative real part which result in stability of system described by (4.19). Condition (4.26) will hold if $\bar{A}$ is Hurwitz. Multiplying (4.26) $X=L^{-1}$ we get (4.27) and simplifying further steps are shown below.

$$L\bar{A} + \bar{A}^{T}L < 0 \tag{4.26}$$

$$\bar{A}X + X\bar{A}^{T} < 0 \tag{4.27}$$

$$(A - BJ)X + X(A - BJ)^{T} < 0 \tag{4.28}$$

$$AX - BJX + XA^{T} - (JX)^{T}B^{T} < 0 \tag{4.29}$$

With J and X are designed as symmetric matrices.

CHAPTER 5: RESULTS & SIMULATION

All simulations are performed in Mat-lab. Simulink and Mat-lab both are utilized for analysis. Functional block diagram is designed in Simulink while code is written for m-file. Both are linked using S-Functions. Simulation time is selected as 60 seconds. Separate analysis is performed on both types of payloads as well as helicopter. Results of all three analyses are shown below in following subsections.

5.1 Analysis of Helicopter

This analysis shows result of both Heading-Heave subsystem as well as Longitudinal-Lateral subsystem. These simulations are based on the work of Xian [15] as shown in chapter 3.

5.1.1 Heading-Heave Subsystem

During this analysis to achieve hovering condition helicopter model is given constant vertical height as desired signal then due to control input helicopter start from zero vertical velocity then it increases till desired velocity after that it becomes constant.

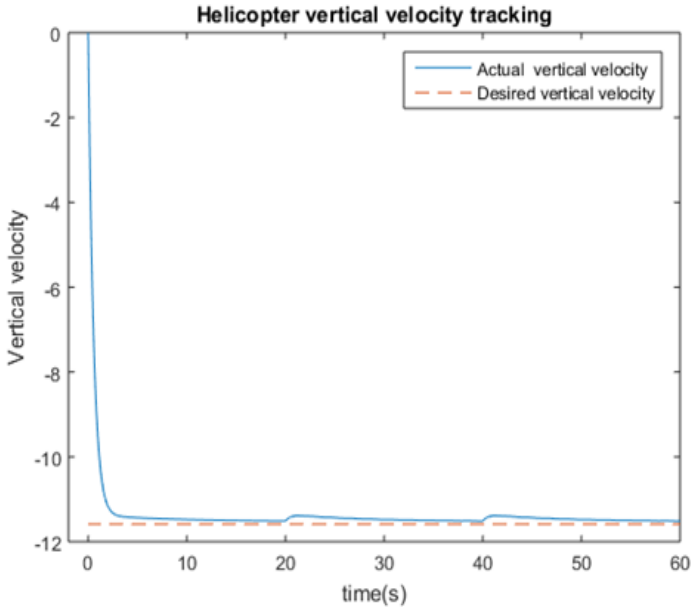

Figure 5.1: Helicopter vertical velocity tracking.

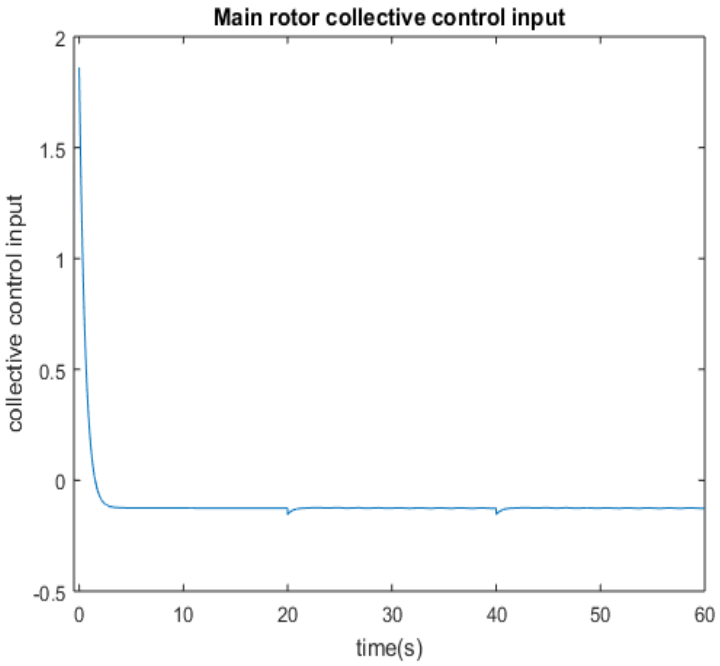

Figure 5.2: Helicopter collective control input.

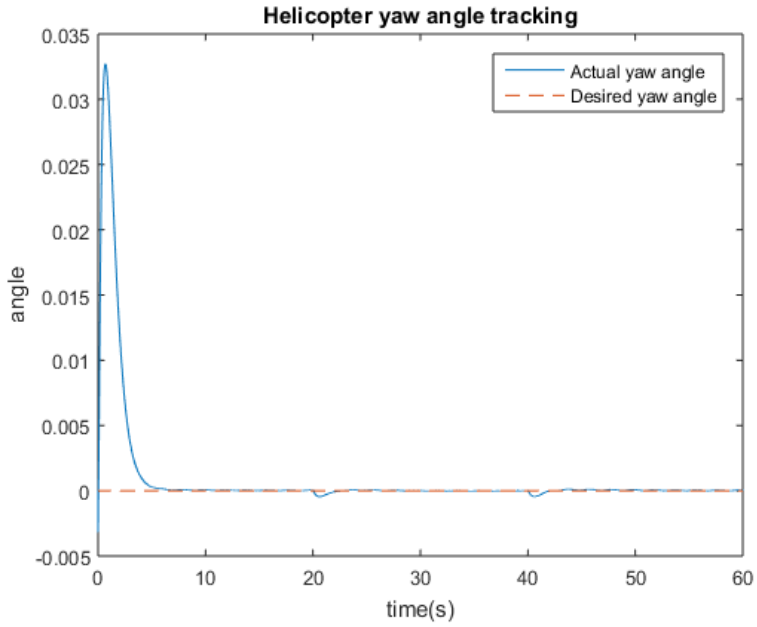

Figure 5.3: Helicopter yaw angle tracking.

Vertical velocity is negative due to the fact that positive vertical axis (z-axis) is chosen downward hence moving upwards requires negative velocity. Figure 5.1 show vertical velocity tracking. Figure 5.2 shows collective control input which is require to track vertical velocity hence it is used to attain vertical height. Figure 5.3 shows yaw angle tracking. As a

condition of hovering yaw angle is kept zero to maintain straight direction. From the figure it is evident that initially yaw angle is not zero but after few seconds it becomes zero.

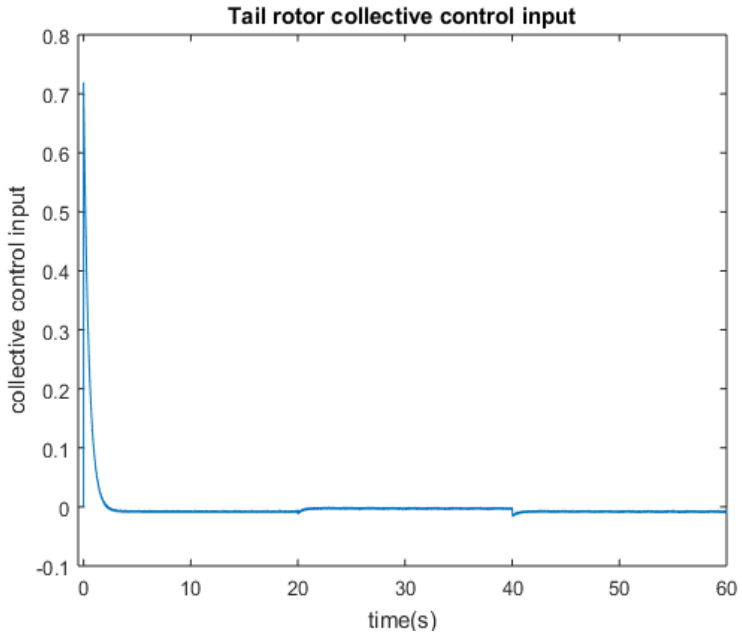

Figure 5.4: Helicopter tail rotor collective control input.

Above shown figure show control input required for achieving yaw angle. Initially control input is non-zero due to the fact that yaw angle initially is not zero after that yaw angle control input becomes zero. Figure 5.5 show heading-heave subsystem Simulink model. Simulink model consists of S-Function blocks which are link between m. files (which contain model as well as code for controlling system) and Simulink. Mux are used to combine data while de-mux split data lines into several one. Some of variables are sent back to workspace (Mat-lab) for analyzing. Integrators are used depending upon logic of equations used in controller designing. Simulation time is selected as 60 seconds and conclusions are drawn on the basis of this lapse of time. Constants used while designing controller are listed in following table.

Table 5.1 Heading-Heave Subsystem Constants

Constant	**Value**
N_v	1
N_p	1
N_w	1
N_r	1

k_3	2
β_3	0.4
λ_3	10
Z_{col}	-50
Z_w	0.75
Z_r	0.75
β_4	0.4
k_p	8
k_i	1
Д1	0.1
Д2	0.1

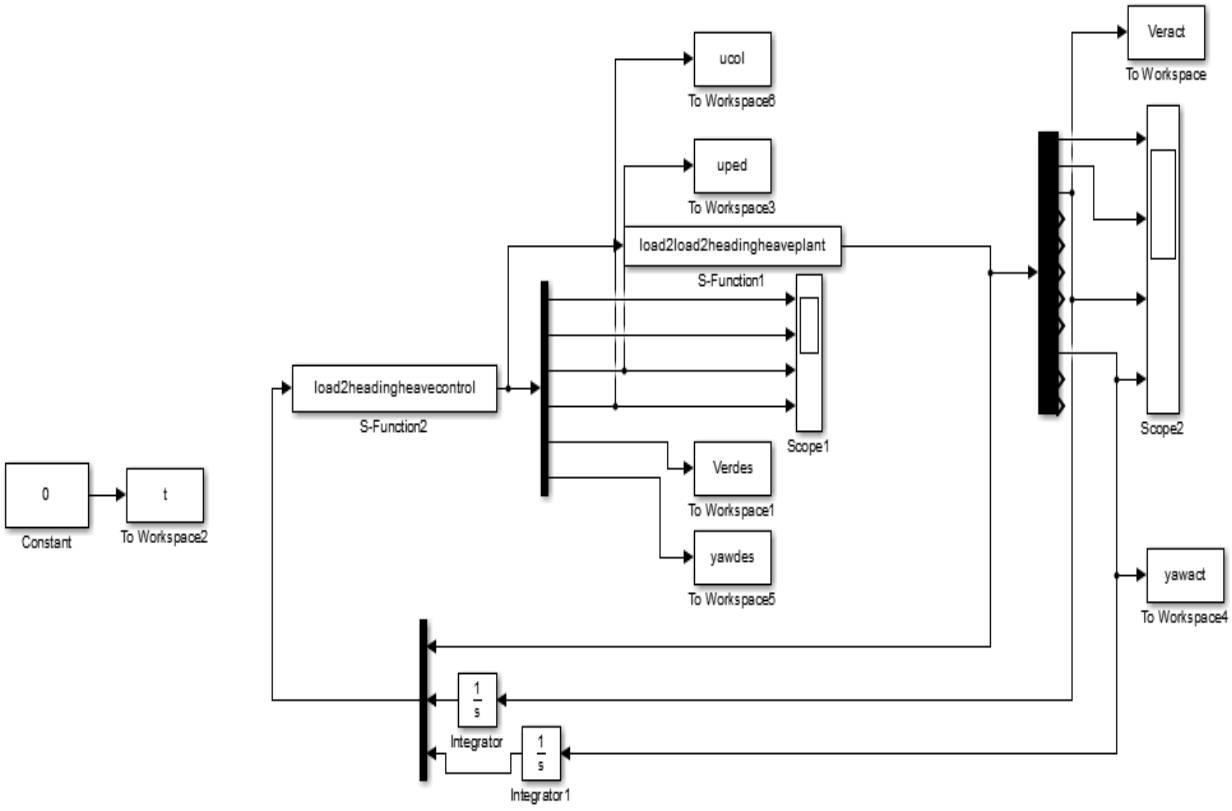

Figure 5.5: Heading-Heave Simulink model.

In order to avoid chattering sat(s) function is adopted instead of sgn(s) function which is defined as following.

$$\text{sat(s)} = \begin{cases} +1, & \text{s} > Д \\ \text{ks}, & |s| \leq Д, \quad k = 1/Д \\ -1, & \text{s} < -Д \end{cases}$$

5.1.2 Longitudinal-Lateral Subsystem

During this analysis to achieve hovering condition helicopter model is given constant longitudinal velocity as well as constant lateral velocity to track. Desired input signal is chosen zero so that helicopter remain stationary.

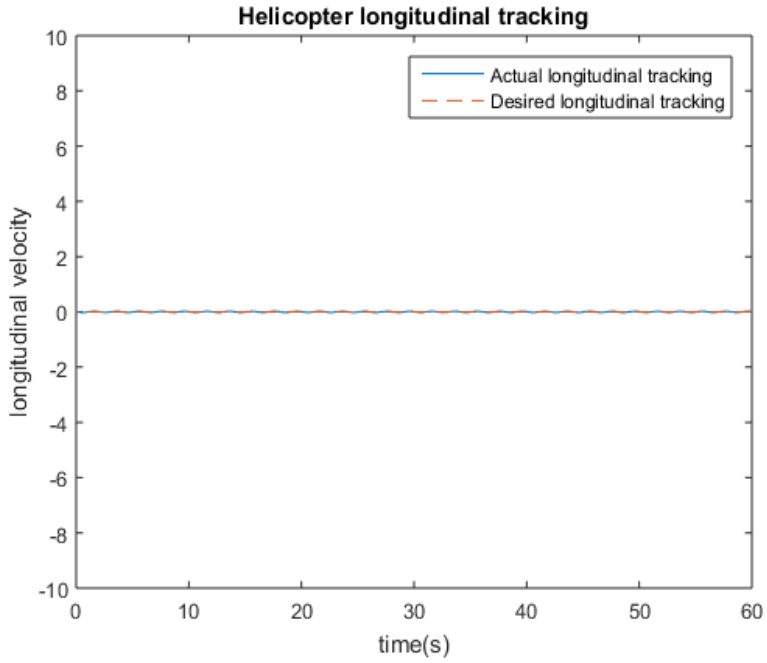

Figure 5.6: Helicopter longitudinal velocity tracking

Figure 5.6 shows helicopter longitudinal tracking response. From this figure it is evident that helicopter tries to keep itself on fix in longitudinal direction. Figure 5.7 show required input to achieve desired response. u_{long} is responsible for controlling longitudinal direction of helicopter. Figure 5.8 show lateral tracking response. This response is similar to as of longitudinal tracking response. It also fluctuates about hovering position. Figure 5.9 show required control input for lateral tracking. Figure 5.10 Simulink model for this subsystem. Table 5.2 shows constants used in this control.

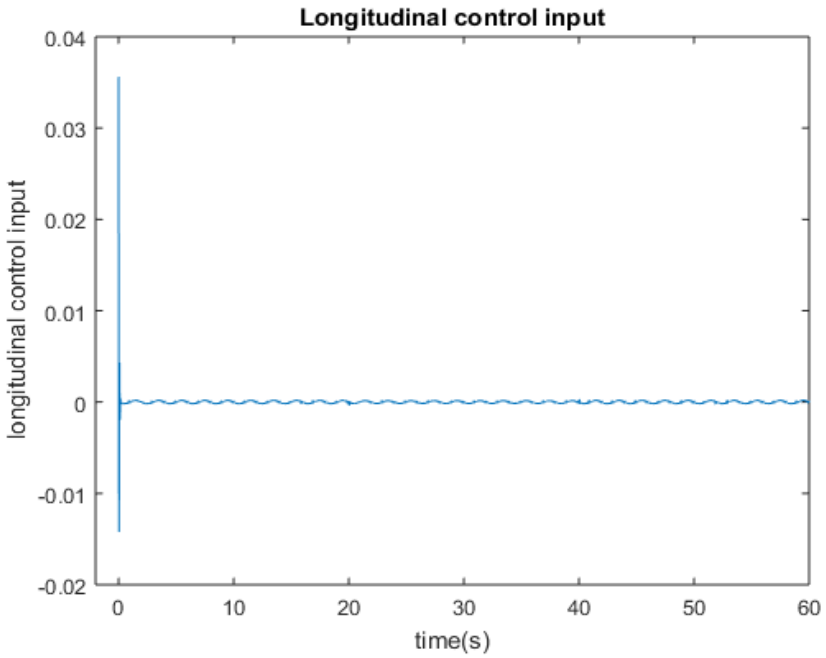

Figure 5.7: Helicopter longitudinal control input

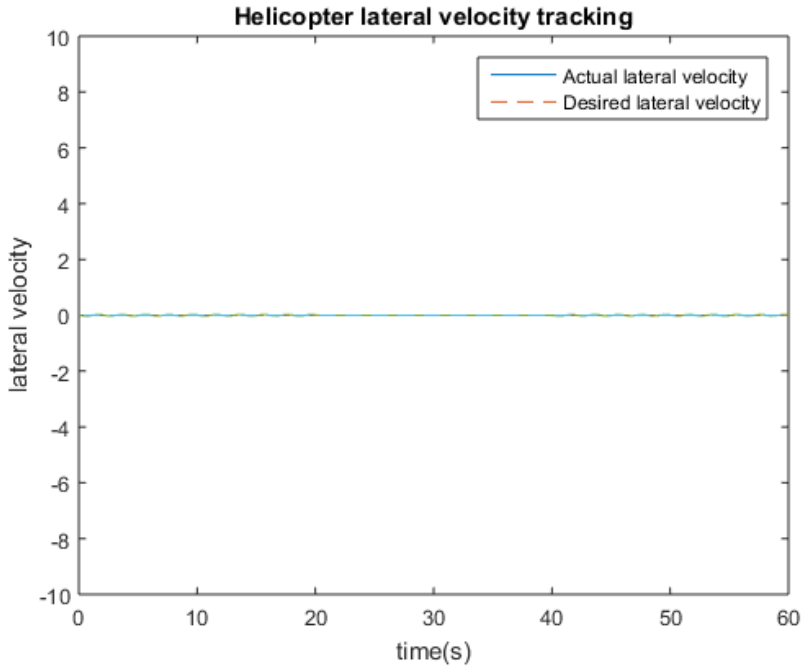

Figure 5.8: Helicopter lateral velocity tracking

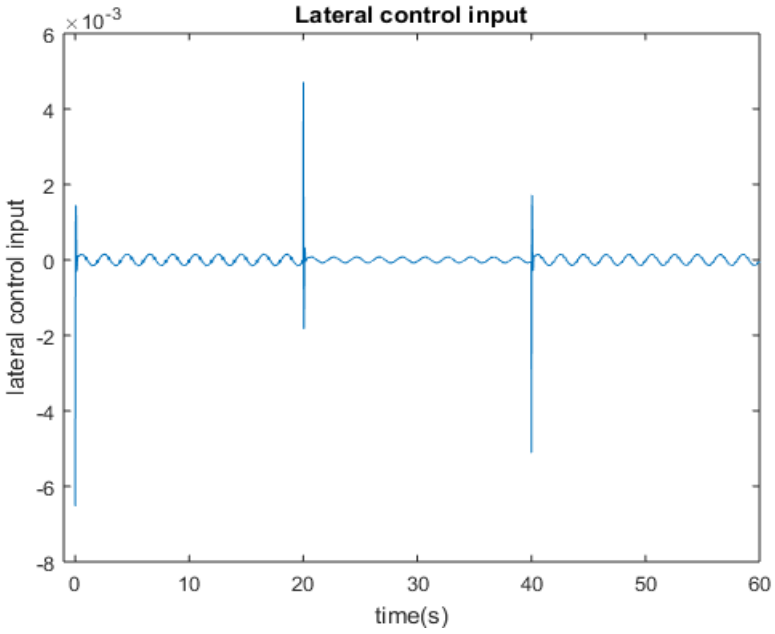

Figure 5.9: Helicopter lateral control input

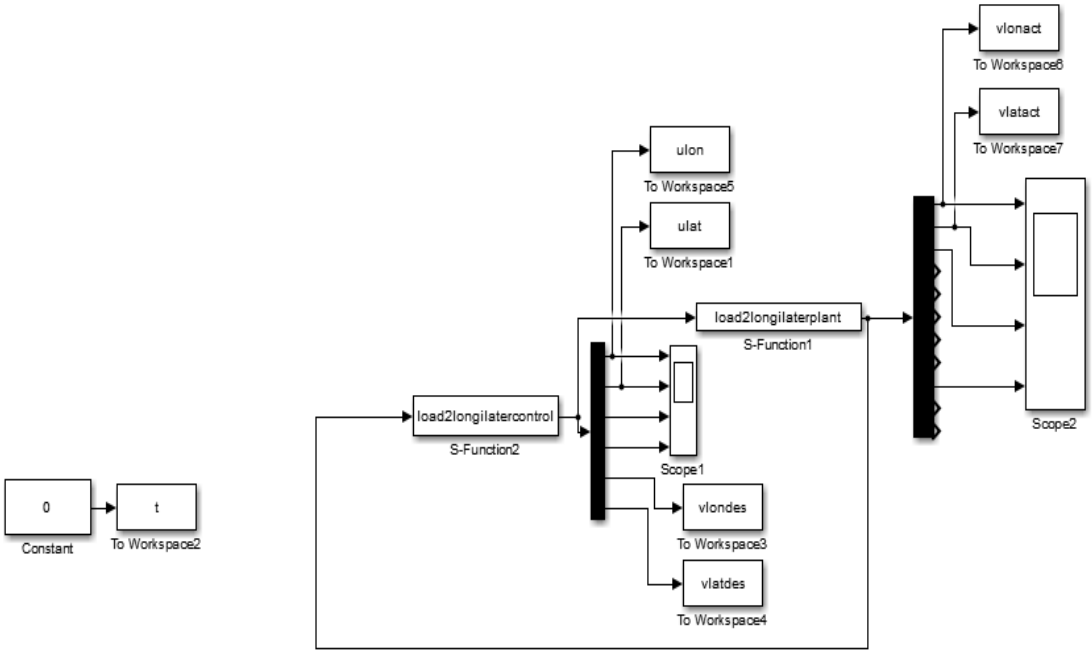

Figure 5.10: Longitudinal-Lateral Simulink model.

Table 5.2 Longitudinal-Lateral Subsystem Constants

Constant	Value
X_u	-0.03996
Y_v	-0.05989
M_u	0.2542
M_v	-0.06013
M_a	307.571
L_u	-0.0244
L_v	-0.1173
L_b	1172.4817
B_a	2.448
A_b	2.233
A_{long}	2.575
B_{lat}	2.575
ζ_f	0.299
β_1	5
β_2	5
k_1	12
k_2	10
λ_1	12
λ_2	10
Д1	0.5
Д2	0.5

5.2 Analysis of Payload

This analysis is based on model proposed by Adams in [11] and control scheme described in chapter 4. It is assumed that helicopter has achieved hovering condition using control scheme proposed for helicopter. After that analysis is performed for both payload models separately and their results are shown for each system in separate sections.

5.2.1 Payload Model 1 Simulations

This section describes stabilization of all states of payload model described by equation (4.1). Figure 5.11 shows payload deflection angle stabilization. Figure 5.12 shows deflection rate stabilization.

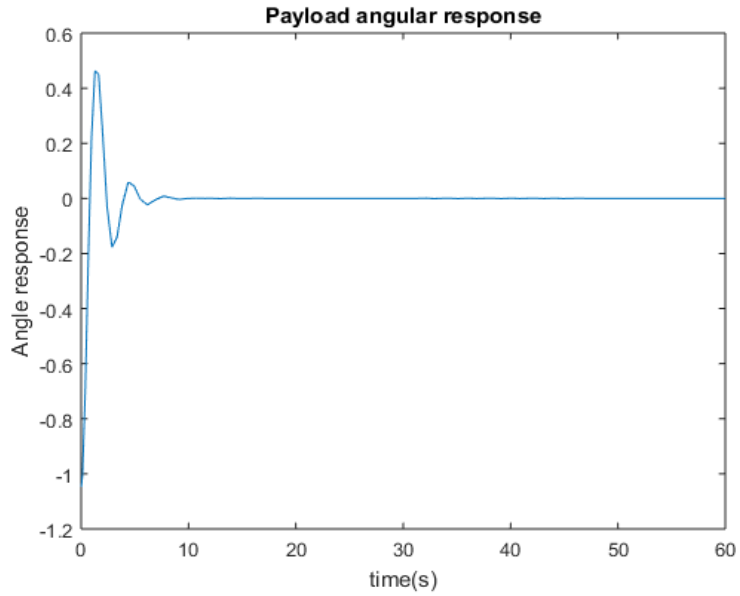

Figure 5.11: Payload deflection angle stabilization.

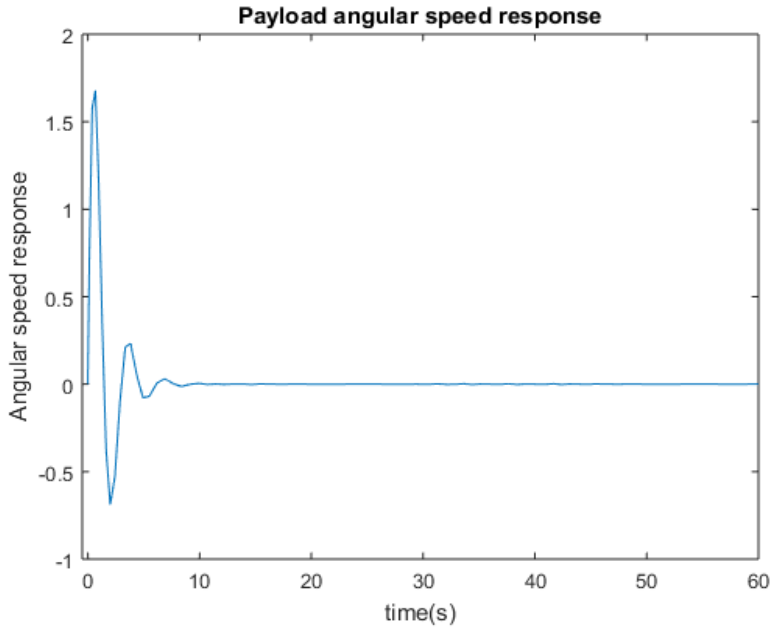

Figure 5.12: Payload deflection rate stabilization.

Figure 5.13 shows helicopter lateral position stabilization. Figure 5.14 shows lateral velocity stabilization. These two responses differs from previous section responses for helicopter in a way that this response is generated after hovering is achieved while previous response is generated to achieve hovering condition.

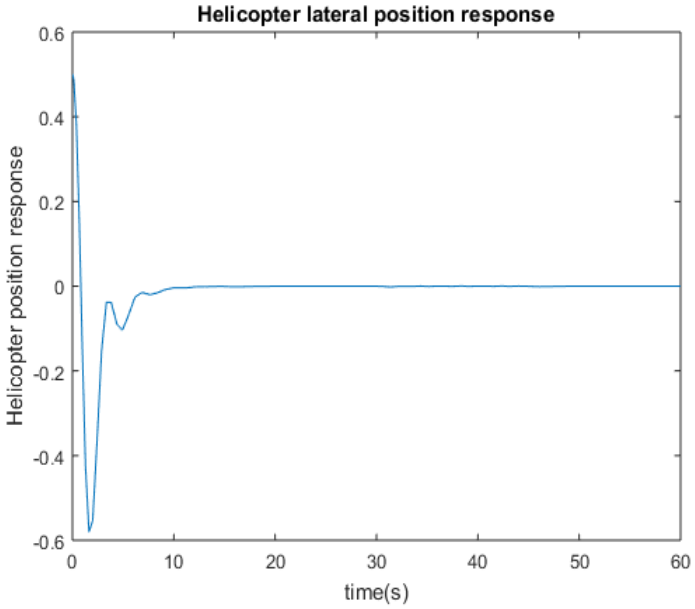

Figure 5.13: Helicopter lateral position stabilization.

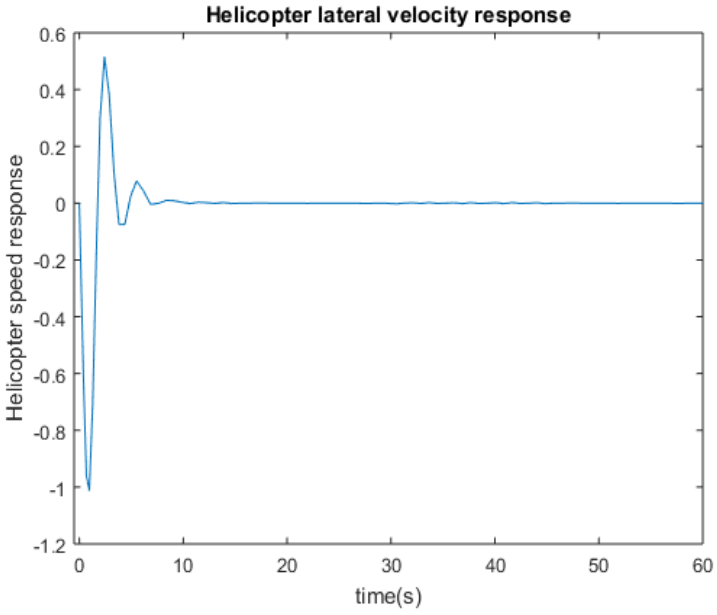

Figure 5.14: Helicopter lateral velocity stabilization.

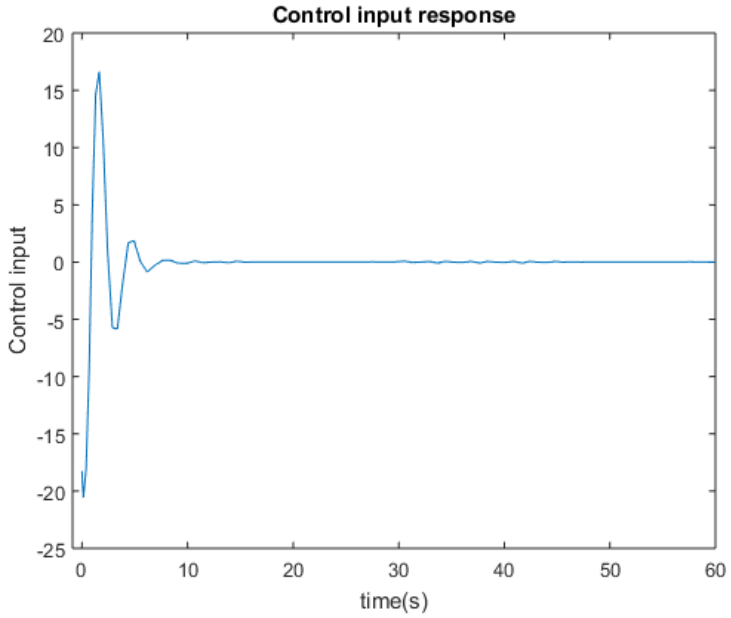

Figure 5.15: Control input for payload stabilization u_{lat}.

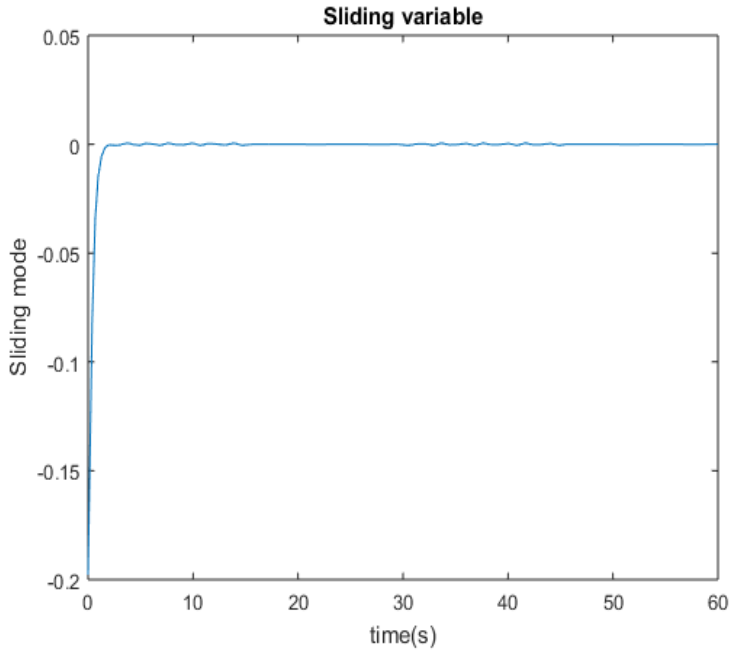

Figure 5.16: Sliding variable (s) response.

Figure 5.15 shows lateral control input. Figure 5.16 shows sliding variable response. Table 5.3 show constants used in developing such control scheme. Figure 5.17 Simulink model of payload subsystem. Values of L and J matrices are described below.

Table 5.3 Payload Subsystem 1 Constants

Constant	Value
$y(0)$	0.5 m
$\dot{y}(0)$	0 m/s
$\alpha(0)$	-60^{o}
$\dot{\alpha}(0)$	0 deg/s
M	9.5 kg
M	0.5 kg
L	1.5 m
D_H	0.8
D_P	0.5
ζ_{max}	0.1
ε_0	0.3
Д	0.1

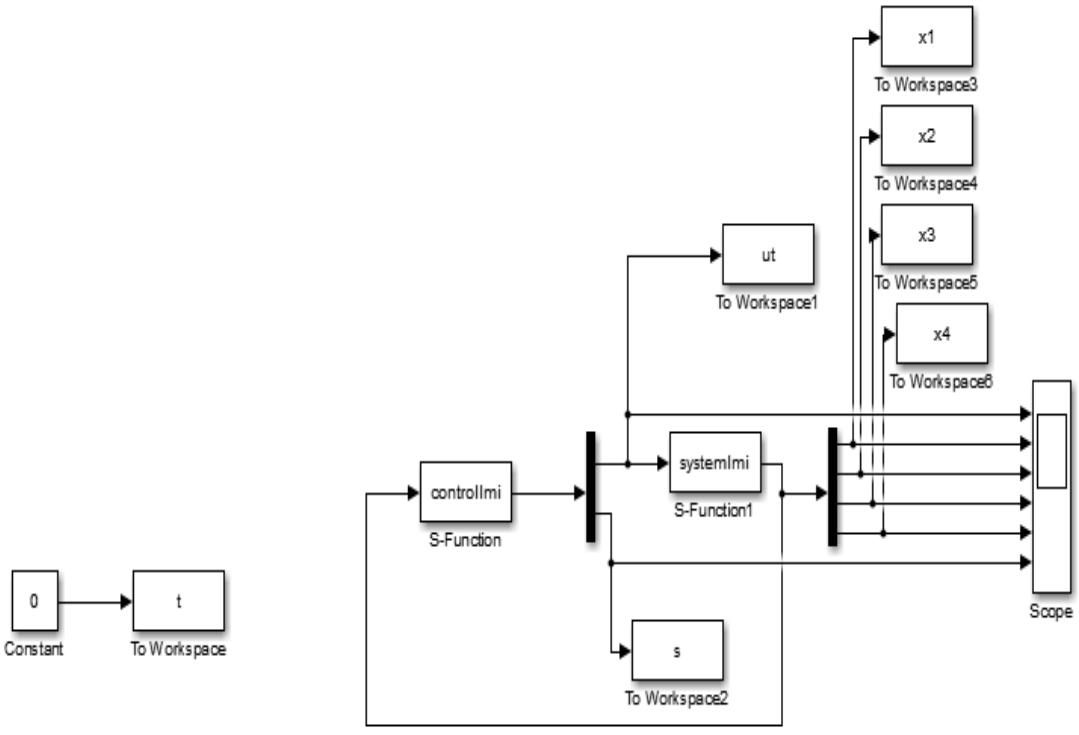

Figure 5.17: Simulink model of payload.

$$L = \begin{bmatrix} 5.7155 & 1.0083 & 1.0923 & 1.4440 \\ 1.0083 & 0.8094 & 0.1537 & 0.2835 \\ 1.0923 & 0.1537 & 1.0891 & 0.5725 \\ 1.4440 & 0.2835 & 0.5725 & 1.2620 \end{bmatrix}$$

$$J = [21.1756 \quad 11.7410 \quad 16.6777 \quad 14.9494]$$

5.2.2 Payload Model 2 Simulations

This section describes stabilization of all states of payload model described by equation (4.2). Figure 5.18 shows helicopter longitudinal displacement stabilization. Table 5.4 show constants used in developing such control scheme and equation (2.43). Figure 5.19 shows helicopter longitudinal velocity stabilization.

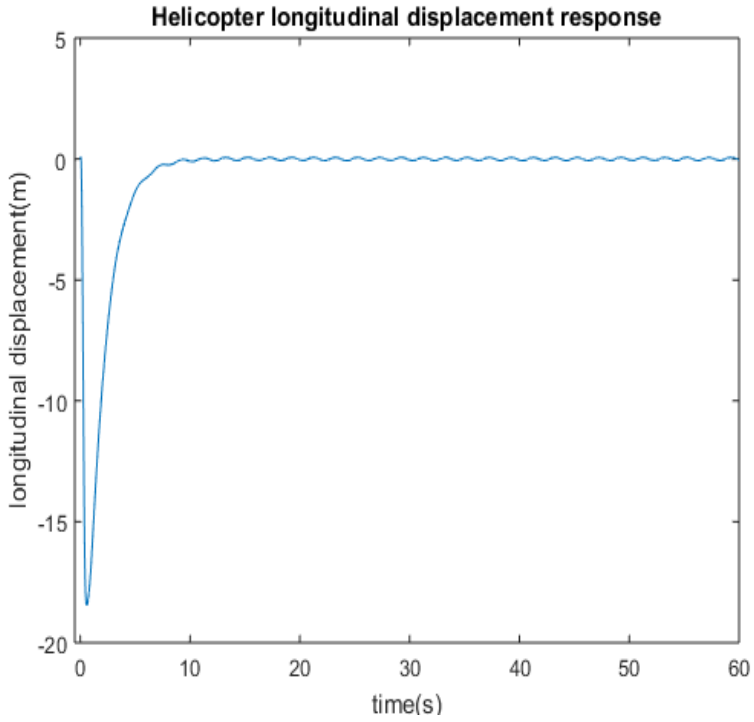

Figure 5.18: Helicopter longitudinal displacement stabilization.

Table 5.4 Payload Subsystem 2 Constants

Constant	Value
$x(0)$	0 m
$\dot{x}(0)$	0 m/s
$\theta(0)$	0^o
$\dot{\theta}(0)$	0 deg/s

$\beta(0)$	-60^{o}
$\dot{\beta}(0)$	0 deg/s
M	9.5 kg
m	0.5 kg
L	1.2 m
c	3.60
d	0.18
x_a	0
y_a	0.08
x_r	0
y_r	0.13
K_m	95.36
B_m	104.9
F	1000 N
r	0.75 m
ρ	1.225 kg/m^3
ζ_{max}	0.1
ε_0	1
Д	25

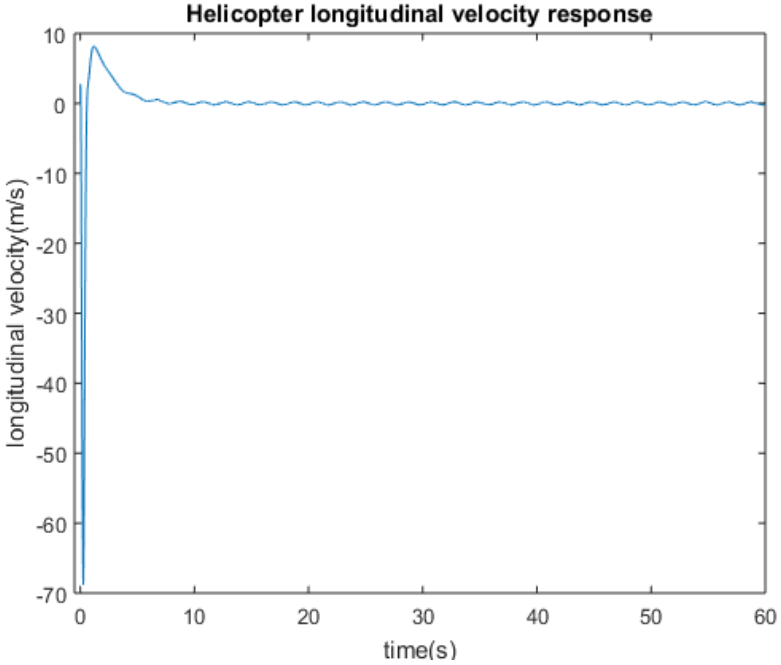

Figure 5.19: Helicopter longitudinal velocity stabilization.

Figure 5.20 shows helicopter pitch angle stabilization and figure 5.21 shows pitch rate stabilization. Value of I_G used is described below.

$$I_G = 0.548 \text{ kg m}^2$$

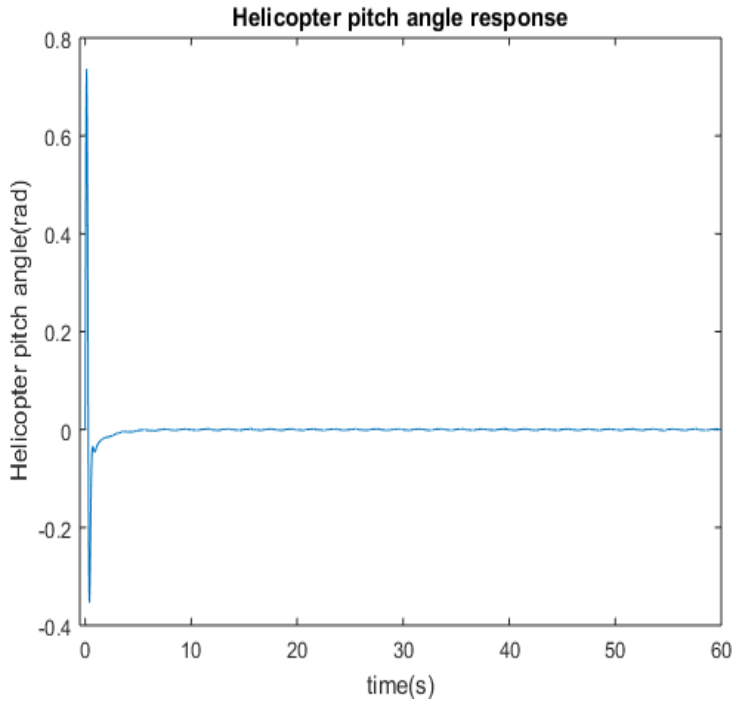

Figure 5.20: Helicopter pitch angle stabilization.

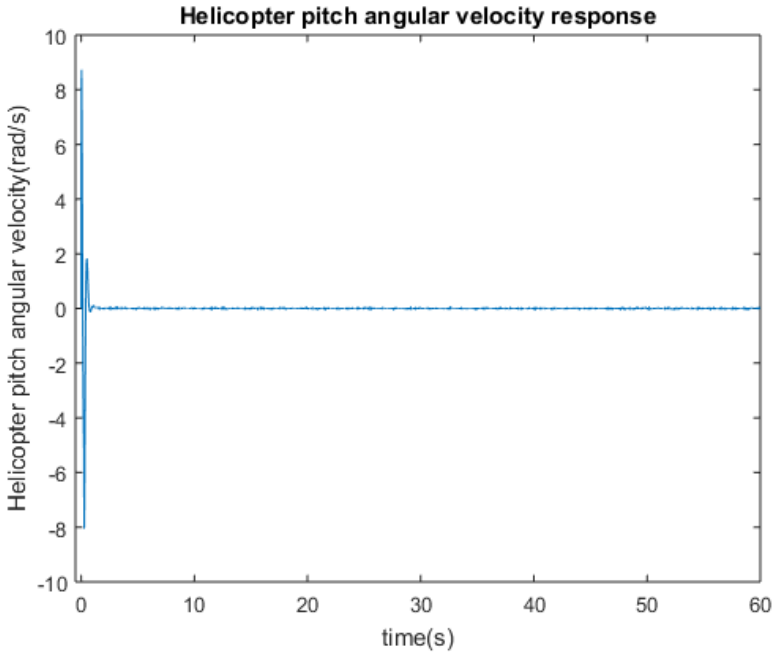

Figure 5.21: Helicopter pitch rate stabilization.

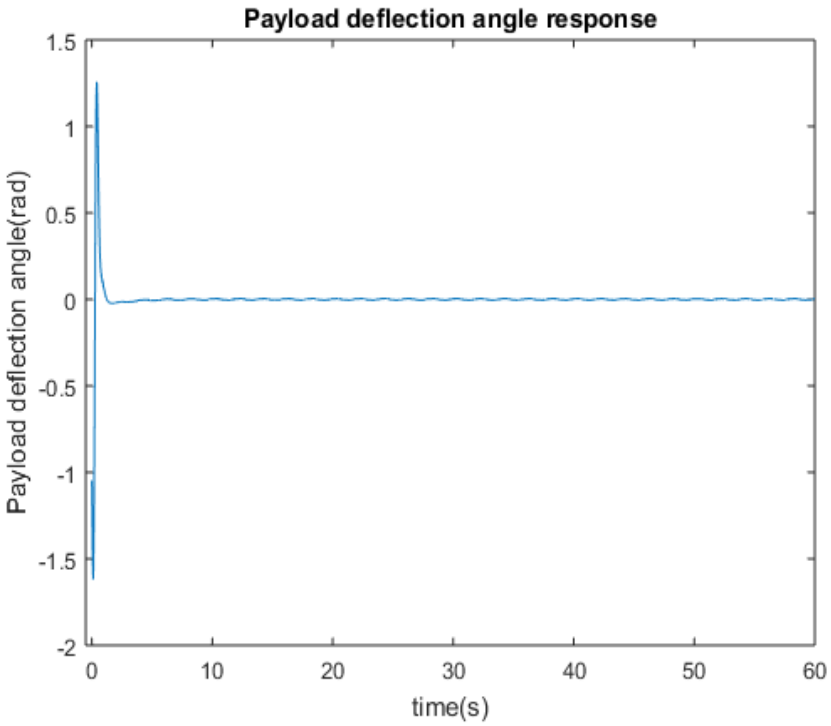

Figure 5.22: Payload deflection angle stabilization.

Figure 5.22 shows payload deflection angle stabilization and figure 5.23 shows payload deflection rate stabilization. Figure 5.24 control input response while figure 5.25 shows sliding variable response.

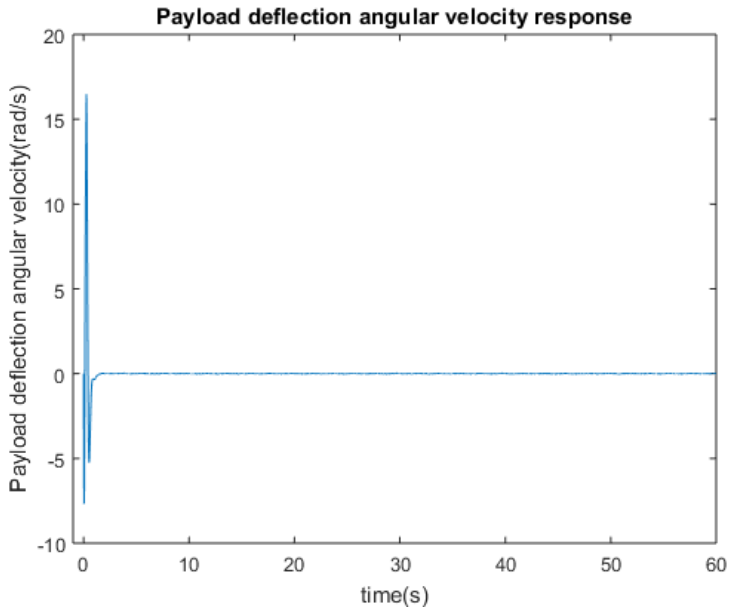

Figure 5.23: Payload deflection rate stabilization.

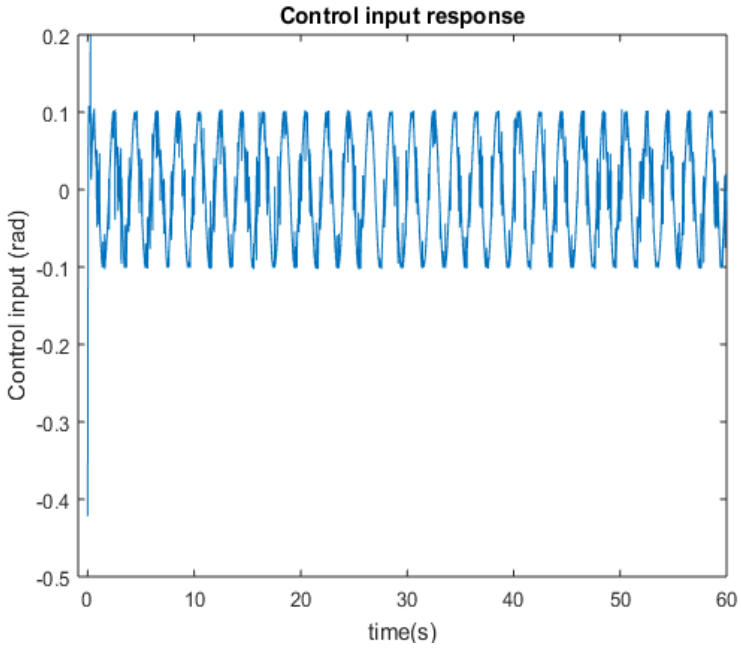

Figure 5.24: Control input.

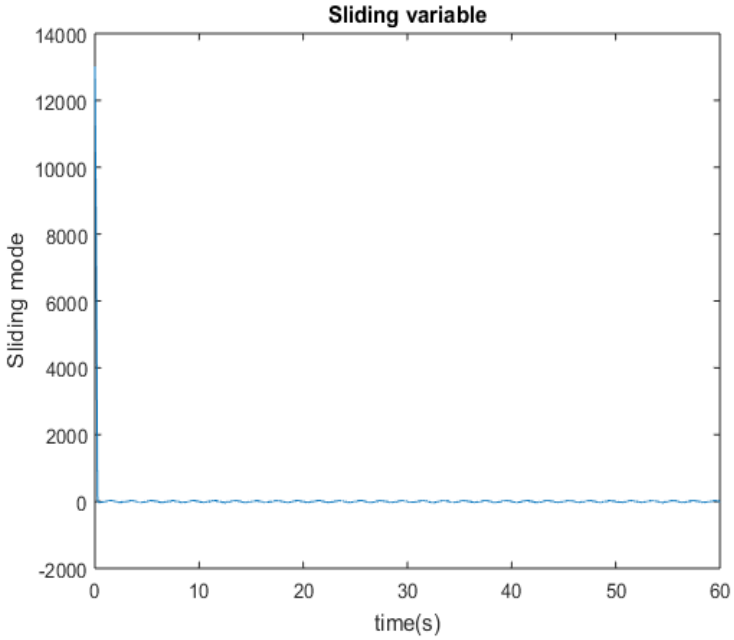

Figure 5.25: Sliding variable (s) response.

Figure 5.26 shows Simulink model for the system. Calculated value of matrix L is also listed below.

$$L = \begin{bmatrix} 0.0401 & 0.0558 & 4.7086 & 0.1156 & 2.7998 & 0.2190 \\ 0.0558 & 0.1718 & 14.8670 & 0.3576 & 8.4860 & 0.6660 \\ 4.7086 & 14.8670 & 1581.6740 & 36.1034 & 864.1172 & 62.4243 \\ 0.1156 & 0.3576 & 36.1034 & 0.8962 & 20.1791 & 1.5420 \\ 2.7998 & 8.4860 & 864.1172 & 20.1791 & 487.7154 & 35.6399 \\ 0.21906 & 0.6660 & 62.4243 & 1.5420 & 35.6399 & 2.7910 \end{bmatrix}$$

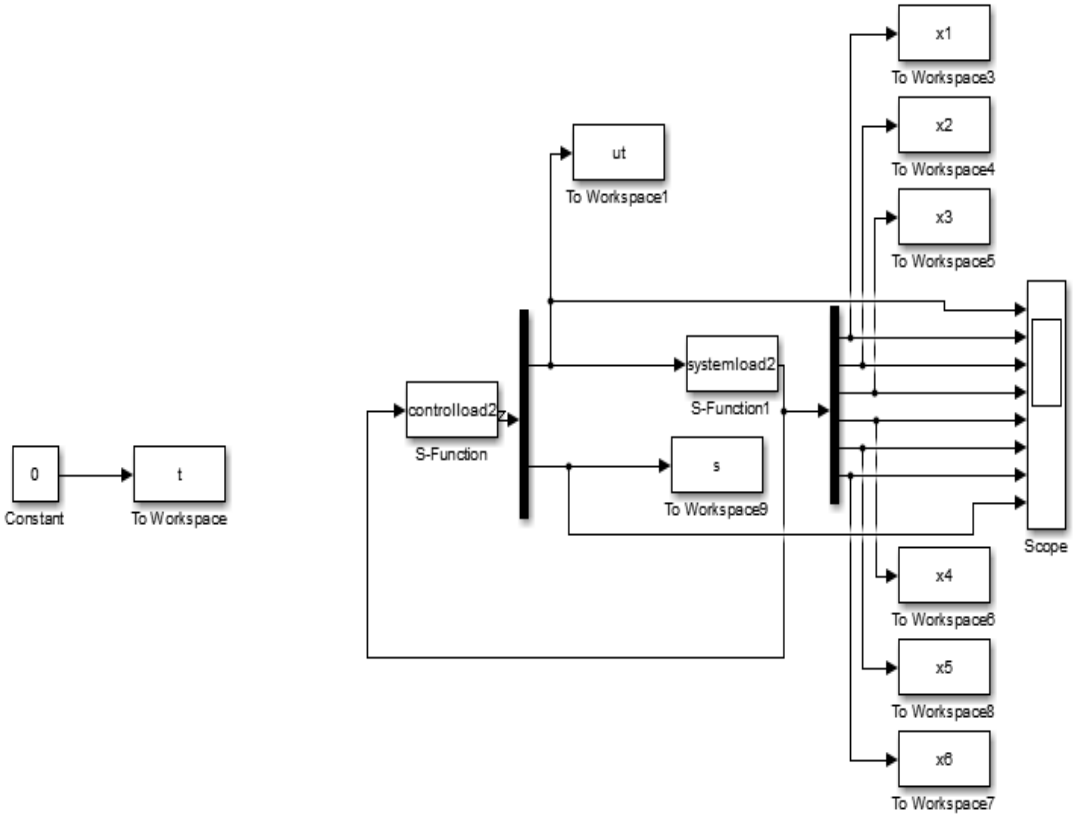

Figure 5.26: Simulink model.

CHAPTER 6: CONCLUSION AND FUTURE WORK

CONCLUSION

In spite of better maneuvering applications of helicopters with suspended load they are more prone to vibrations because of load behavior. Load act as pendulum resulting in disturbing the control of helicopter and distracting the stability of helicopter. In this research, Linear Matrix Inequality based Sliding Mode Control is proposed for stabilizing payload suspended with helicopter in the presence of external disturbances. These disturbances include rotor downwash effects as well as air disturbances. Helicopter is given pre-defined trajectory and is given command to track it. Satisfactory results of helicopter tracking are obtained using Sliding Mode Control based on linearized dynamics. Once helicopter has achieved hovering analysis on payload is performed. From results it is evident that payload is stabilized effectively in the presence of disturbances.

FUTURE WORK

- Similar analysis can be performed for forward flight case.
- Better coupling can be developed that will remain valid for both forward as well as hovering condition of helicopter.
- Sliding mode control based on nonlinear dynamics and nonlinear model can be analyzed.

BIBLIOGRAPHY

[1] H. Liu, G. Lu and Y. Zhong, "Robust LQR Attitude Control of a 3-DOF Laboratory Helicopter for Aggressive Maneuvers", IEEE Transactions on Industrial Electronics, vol. 60, no. 10, pp. 4627-4636, 2013.

[2] Jongho Shin, Kim, H., Youdan Kim and Dixon, W. (2012). Autonomous Flight of the Rotorcraft-Based UAV Using RISE Feedback and NN Feedforward Terms. *IEEE Transactions on Control Systems Technology*, 20(5), pp.1392-1399.

[3] Cai, G., Chen, B., Dong, X. and Lee, T. (2011). Design and implementation of a robust and nonlinear flight control system for an unmanned helicopter. *Mechatronics*, 21(5), pp.803-820.

[4] Raptis, I., Valavanis, K. and Vachtsevanos, G. (2012). Linear Tracking Control for Small-Scale Unmanned Helicopters. *IEEE Transactions on Control Systems Technology*, 20(4), pp.995-1010.

[5] C. J Adams, "Modeling and control of helicopters carrying suspended loads", Georgia Institute of Technology, Atlanta, Georgia, 2012.

[6] Raptis, I., Valavanis, K. and Moreno, W. (2011). A Novel Nonlinear Backstepping Controller Design for Helicopters Using the Rotation Matrix. *IEEE Transactions on Control Systems Technology*, 19(2), pp.465-473.

[7] T. Dukes, "Maneuvering Heavy Sling Loads Near Hover Part II: Some Elementary Maneuvers", Journal of the American Helicopter Society, vol. 18, no. 3, pp. 17-22, 1973.

[8] Stevens, B., Lewis, F. and Johnson, E. (1992). *Aircraft control and simulation*. NJ:John Wiley & Sons,Inc., pp.421-437.

[9] M. Bisgaard, A. Cour-Harbo, and J. D. Bendtsen. Full state estimation for helicopter slung load system. In AIAA Guidance, Navigation, and Control Conf., volume 4, pages 4036–4050, Hilton Head,SC, 2007.

[10] J. A. Ottander and E. N. Johnson. Precision slung cargo delivery onto a moving platform. In AIAA Modeling and Simulation Technologies Conf., Toronto, Canada, 2-5 August 2010.

[11] C. Adams, J. Potter and W. Singhose, "Modeling and input shaping control of a micro coaxial radio-controlled helicopter carrying a suspended load", in *2012 12th International Conference on Control, Automation and Systems (ICCAS).*, JeJu Island, South Korea, 2012, pp. 645-650.

[12] Y. Guo, Z. Zheng, M. Zhu and Z. Wu, "Neural network tracking control of the 3-DOF helicopter with input saturation", in *2016 Chinese Control and Decision Conference (CCDC)*, Yinchuan, China, 2016, pp. 2656-2660.

[13] B. Hanson, "Investigation of a non-uniform helicopter rotor downwash model", Linkoping University, Linkoping, 2008.

[14] H. Johansson, "Investigation of rotor downwash effects using CFD", Linkoping University, Linkoping, 2009.

[15] B. Xian, G. Jianchuan, Z. Yao and Z. Bo, "Sliding mode tracking control for miniature unmanned helicopters", *Chinese Journal of Aeronautics*, vol. 28, no. 1, pp. 277-284, 2015.

[16] T. Koo and S. Sastry, "Output tracking control design of a helicopter model based on approximate linearization", in *37th IEEE Conference on Decision and Control, 1998*, Tampa, FL, USA, 1998, pp. 3636-3640.

[17] J. Potter, C. Adams and W. Singhose, "A Planar Experimental Remote-Controlled Helicopter With a Suspended Load", IEEE/ASME Transactions on Mechatronics, vol. 20, no. 5, pp. 2496-2503, 2015.

[18] J. Liu and X. Wang, Advanced sliding mode control for mechanical systems. Beijing: Tsinghua University, 2012, pp. 81-83.

[19] V. Leu, H. Choi and J. Jung, "LMI-based Sliding Mode Speed Tracking Control Design for Surface-mounted Permanent Magnet Synchronous Motors", *Journal of Electrical Engineering and Technology*, vol. 7, no. 4, pp. 513-523, 2012.

[20] F. Gouaisbaut, M. Dambrine and J. Richard, "Robust control of delay systems: a sliding mode control design via LMI", *Systems & Control Letters*, vol. 46, no. 4, pp. 219-230, 2002.

COMPLETION CERTIFICATE

"It is certified that the contents of thesis document titled "*Adaptive Sliding Mode Control for Suspended Payload with Helicopter"* submitted by Mr. Hassaan Afzal Registration No. 00000118999 have been found satisfactory for the requirement of degree".

Thesis Advisor: _____

(Dr. Fahad Mumtaz Malik)